



## RESEARCH PAPER

# Methyl jasmonate-induced emission of biogenic volatiles is biphasic in cucumber: a high-resolution analysis of dose dependence

Yifan Jiang<sup>1,2</sup>, Jiayan Ye<sup>1</sup>, Shuai Li<sup>1</sup> and Ülo Niinemets<sup>1,3,\*</sup>

<sup>1</sup> Institute of Agricultural and Environmental Sciences, Estonian University of Life Sciences, Kreutzwaldi 1, Tartu 51014, Estonia

<sup>2</sup> College of Art, Changzhou University, Gehu 1, Changzhou 213164, Jiangsu, China

<sup>3</sup> Estonian Academy of Sciences, Kohtu 6, 10130 Tallinn, Estonia

\* Correspondence: [ylo.niinemets@emu.ee](mailto:ylo.niinemets@emu.ee)

Received 4 January 2017; Editorial decision 24 June 2017; Accepted 25 June 2017

Editor: Peter Bozhkov, Swedish University of Agricultural Sciences

## Abstract

**Methyl jasmonate (MeJA) is a key airborne elicitor activating jasmonate-dependent signaling pathways, including induction of stress-related volatile emissions, but how the magnitude and timing of these emissions scale with MeJA dose is not known. Treatments with exogenous MeJA concentrations ranging from mild (0.2 mM) to lethal (50 mM) were used to investigate quantitative relationships among MeJA dose and the kinetics and magnitude of volatile release in *Cucumis sativus* by combining high-resolution measurements with a proton-transfer reaction time-of-flight mass spectrometer (PTR-TOF-MS) and GC-MS. The results highlighted biphasic kinetics of elicitation of volatiles. The early phase, peaking in 0.1–1 h after the MeJA treatment, was characterized by emissions of lipoxygenase (LOX) pathway volatiles and methanol. In the subsequent phase, starting in 6–12 h and reaching a maximum in 15–25 h after the treatment, secondary emissions of LOX compounds as well as emissions of monoterpenes and sesquiterpenes were elicited. For both phases, the maximum emission rates and total integrated emissions increased with applied MeJA concentration. Furthermore, the rates of induction and decay, and the duration of emission bursts were positively, and the timing of emission maxima were negatively associated with MeJA dose for LOX compounds and terpenoids, except for the duration of the first LOX burst. These results demonstrate major effects of MeJA dose on the kinetics and magnitude of volatile response, underscoring the importance of biotic stress severity in deciphering the downstream events of biological impacts.**

**Key words:** Biotic stress, cucumber, dose–response, LOX products, MeJA, proton-transfer reaction time-of-flight mass spectrometer (PTR-TOF-MS), terpenes.

## Introduction

Endogenous levels of jasmonic acid (JA) and its methylated derivative methyl jasmonate (MeJA) are known to increase rapidly in response to herbivore attack or invasion by pathogens, subsequently activating downstream defense responses. Once released into the air, MeJA has been shown to act as

a long-distance airborne signal to trigger defense responses in non-impacted parts of the damaged plant or in neighboring plants (Heil and Ton, 2008; Tamogami *et al.*, 2008; Cheong and Choi, 2003). Thus, exogenous application of MeJA has often been used to simulate the impact of a biotic

stress on elicitation of jasmonate-dependent defenses (Zhao and Chye, 1999; Heijari *et al.*, 2008; Tamogami *et al.*, 2008; Suh *et al.*, 2013; Shi *et al.*, 2015; Jiang *et al.*, 2016a). Among these induced defenses, elicitation of the release of volatile emissions in MeJA-treated leaves is a characteristic MeJA response (Dicke *et al.*, 1999; Kappers *et al.*, 2010; Mäntylä *et al.*, 2014). The chemical classes of plant volatile blends induced by MeJA vary considerably in quantity, quality, and timing, with green leaf volatiles [lipoxygenase (LOX) compounds] and various terpene compounds (mainly monoterpenes and sesquiterpenes) being the typical elicited volatiles (Rodriguez-Saona *et al.*, 2001; Martin *et al.*, 2003; Semiz *et al.*, 2012; Kegge *et al.*, 2013). These emissions occur as the result of both constitutive activity of key stress pathways (e.g. constitutive LOX activities leading to rapid emission of green leaf volatiles; Andreou and Feussner, 2009) and activation of expression of genes responsible for specialized volatile synthesis (e.g. elicitation of expression of terpene synthases leading to emissions of mono- and sesquiterpenes; Martin *et al.*, 2002, 2003; Byun-McKay *et al.*, 2006). Despite the diversity, these induced emissions resemble the emissions induced by herbivores or by physical wounding, and can serve as infochemicals in attracting herbivore enemies or in priming defenses in neighboring plants (Dicke *et al.*, 1999; Heil and Kost, 2006; Heil and Ton, 2008; Kappers *et al.*, 2010), thus underscoring the biological significance of MeJA as a model of chemical signaling.

So far, the majority of studies on the relationships of stress-driven volatile emissions and biotic stress, including herbivore infestation and exogenous MeJA application, have been non-quantitative and have not focused on understanding how much is emitted in response to a certain elicitor dose. The studies have rather mainly looked at the modifications in volatile profiles or at the ecological roles of the volatile induction, for example in plant indirect defenses. However, there is encouraging evidence that the stress-dependent elicitation of volatile emissions is linked to the severity of biotic impacts in a dose-dependent manner (Niinemets *et al.*, 2013). The severity of biotic stress has been modified by varying the degree of wounding (Mithöfer *et al.*, 2005; Portillo-Estrada *et al.*, 2015, 2017) or varying the number of feeding larvae (Copolovici *et al.*, 2011; Yli-Pirilä *et al.*, 2016; Copolovici *et al.*, 2017). However, the definition of the severity of biotic stress, the stress ‘dose’, is still difficult in biotic stress studies because of localized spread and complexity of timing of biotic impacts, especially for multiple biotic impacts occurring at somewhat different times, such as simultaneous herbivore feeding and spread of pathogen infections. Such complex impacts can lead to emission responses that are hard to decipher, complicating construction of mechanistic quantitative stress severity versus emission response models for prediction of signaling among neighboring plants and other organisms (Grote *et al.*, 2013). As exogenous MeJA can be applied in precisely defined doses, it can provide an invaluable model system to simulate dose dependencies of biotic impacts, and start resolving complex biological interactions, at least using volatile responses as a quantitative measure of biotic stress severity.

A dose dependence between the exogenous MeJA concentration and plant volatile response can be expected because treatments with a higher concentration probably result in a greater coverage of potential impact sites in cell wall and cellular membrane surfaces. Furthermore, MeJA exposure has also been related to the downstream components of signaling pathways in cell death regulation (Jonak *et al.*, 2002), and studies using higher concentrations of exogenous MeJA have reported hypersensitive responses including necrosis and/or activation of programmed cell death (PCD) (Popova *et al.*, 2003; Jung, 2004; Zhang and Xing, 2008; Repka *et al.*, 2013) that are expected to result in profound modifications in the total amount and profiles of volatile emission (Beauchamp *et al.*, 2005; Niinemets, 2010). Although the evidence suggests that MeJA activates defense pathways in a dose-dependent manner, to our knowledge, the way in which the MeJA dose alters the timing and magnitude of induced volatile responses has not been studied.

We used cucumber (*Cucumis sativus* L.), known to respond strongly to MeJA (Bouwmeester *et al.*, 1999; Kappers *et al.*, 2010), as the model to investigate the effect of different exogenous MeJA concentrations through early and late phases of MeJA response by combining high-resolution measurements with a proton-transfer reaction time-of-flight mass spectrometer (PTR-TOF-MS) and GC-MS measurements, and kinetic analyses (Table 1). We asked how MeJA dose alters the total amount of volatiles released, how it affects volatile composition, and how it modifies the kinetics of volatile release. We hypothesized that there are MeJA dose-dependent differences in the overall degree of elicitation and compositions of induced volatile emissions. The results of the current study highlight biphasic emission kinetics of volatile emission and strong quantitative relationships between MeJA concentration and the timing and magnitude of early and late emission responses.

## Materials and methods

### Plant growth conditions

Cucumber (*Cucumis sativus* cv. Libelle F1, Seston Seemned OÜ, Estonia) seeds were sown in 1 liter plastic pots filled with a mixture (1:1) of sand and commercial potting soil (Biolan Oy, Finland), and cultivated in an environment-controlled plant growth room (Copolovici *et al.*, 2012). In brief, light intensity of 300–400  $\mu\text{mol m}^{-2} \text{s}^{-1}$  at the level of plants was provided for 12 h by Philips HPI/T Plus 400 W metal halide lamps (Philips Eesti, Tallinn, Estonia). Air temperature was 24 °C during the day and 20 °C at night, and relative humidity was maintained at 60–70% through the day and night. Plants were watered daily to field capacity, and fertilized every 3 d with a commercial NPK fertilizer (N-P<sub>2</sub>O<sub>5</sub>-K<sub>2</sub>O: 19-5-13). Approximately 3- to 4-week-old, 20–30 cm tall plants with four to five fully expanded leaves were used in the experiments.

### Methyl jasmonate (MeJA) treatments

As studies have used widely different protocols for MeJA application (e.g. Thaler *et al.*, 2002; Loivamäki *et al.*, 2004; Heijari *et al.*, 2005; Liang *et al.*, 2006; Phillips *et al.*, 2007), we tested different methods in preliminary experiments. These tests included different solvents (water with 0.01% Triton X-100 versus 5% ethanol), mode of treatment (spraying versus brushing), treatment location (ventilated

**Table 1.** Definition of the traits characterizing the kinetics of volatile compounds released upon methyl jasmonate treatment (see Fig. 2 for representative emission kinetics)

Symbol (unit)	Definition
$D_M$ (h)	Duration between the first and the second emission maxima
$D_{P1}$ (h)	Duration of the first induced emission peak
$D_{P2}$ (h)	Duration of the second induced emission peak
$I_{T1}$ (nmol m <sup>-2</sup> )	Integral of the first emission peak (Equation 1)
$I_{T2}$ (nmol m <sup>-2</sup> )	Integral of the second emission peak
$I_{Tot}$ (nmol m <sup>-2</sup> )	Integral of the total induced emissions, $I_{T1}+I_{T2}$
$k_{I1}$ (h <sup>-1</sup> )	Rate constant for the initial increase of emissions during the first emission burst (Equation 2)
$k_{D1}$ (h <sup>-1</sup> )	Rate constant for the decrease of emissions during the first emission burst (Equation 3)
$k_{I2}$ (h <sup>-1</sup> )	Rate constant for the increase of emissions during the second emission burst
$k_{D2}$ (h <sup>-1</sup> )	Rate constant for the decrease of emissions during the second emission burst
$t_{M1}$ (h)	Time to the first emission maximum since the start of the treatment
$t_{M2}$ (h)	Time to the second emission maximum since the start of the treatment
$t_{P1S}$ (h)	Start of the first emission burst since the start of the treatment
$t_{P1E}$ (h)	End of the first emission burst since the start of the treatment
$t_{P2S}$ (h)	Start of the second emission burst since the start of the treatment
$t_{P2E}$ (h)	End of the second emission burst since the start of the treatment
$\tau_{I1}$ (h)	Doubling time for the increase of emissions during the first emission burst
$\tau_{D1}$ (h)	Half-time for the decrease of emissions during the first emission burst
$\tau_{I2}$ (h)	Doubling time for the increase of emissions during the second emission burst
$\tau_{D2}$ (h)	Half-time for the decrease of emissions during the second emission burst
$\Phi(t)$ (nmol m <sup>-2</sup> s <sup>-1</sup> )	Emission rate at time $t$
$\Phi_{M1}$ (nmol m <sup>-2</sup> s <sup>-1</sup> )	Maximum emission rate at the first emission peak
$\Phi_{M2}$ (nmol m <sup>-2</sup> s <sup>-1</sup> )	Maximum emission rate at the second emission peak

hood versus an experimental ventilated flow-through glass chamber; see the details in ‘Dynamic headspace collection of volatiles’). The key selection criteria for MeJA treatment were the repeatability of the treatment in terms of quantitative volatile response and minimization of non-specific effects as assessed by comparing the volatile emissions of non-treated plants and control plants treated with pure solvent identically to the MeJA treatment. Ultimately, application of MeJA (Sigma-Aldrich, St Louis, MO, USA) in 5% aqueous ethanol by spraying in the experimental glass chamber as in several previous studies (Martin *et al.*, 2003; Semiz *et al.*, 2012; Jiang *et al.*, 2016b) was selected as the most repeatable application procedure that was associated with minor non-specific effects in control treatments. In fact, volatile emissions in the control treatment (5% ethanol solution) did not significantly differ from non-treated plants.

To obtain the MeJA dose response, the following concentrations were used: 0 (control, 5% ethanol), 0.2, 2, 5, 10, 20, and 50 mM. The selected leaf with an area of ~40 cm<sup>2</sup> was sealed in the glass gas-exchange cuvette of one of the two gas-exchange systems described below, the baseline measurement of volatile emissions was taken, the cuvette was opened, and 10 ml of MeJA solution was sprayed over the entire leaf surface to obtain a complete and even coating. Immediately after the treatment, the treated leaf was sealed in the gas exchange cuvette again (within ~1 min) and, depending on the system used, volatiles were collected at intervals and analyzed offline by GC-MS or monitored continuously using an online PTR-TOF-MS. Three different plants were used for each MeJA concentration treatment.

#### Dynamic headspace collection of volatiles

Volatile collection for GC-MS analysis was carried out with a multichamber open gas-exchange system described in detail by Toome *et al.* (2010) and Copolovici *et al.* (2011) that was also used for MeJA treatments as described above. Each 3 liter glass chamber was operated individually using purified ambient air for the chamber inlet and maintaining an air flow rate of 1 l min<sup>-1</sup> through the chamber. Turbulent conditions inside the chambers were achieved by a fan

installed at the bottom of each individual chamber. The light regime during measurements followed growth light conditions, with light intensity of 200–400  $\mu\text{mol m}^{-2} \text{s}^{-1}$  provided for 12 h per day with a Heliospectra LX60 plant growth LED lamp (Heliospectra AB, Sweden). The temperature inside the chambers was between 24 and 26 °C during the light period and 22 °C during the dark period, air humidity was ~60%, and CO<sub>2</sub> concentration was 380  $\mu\text{mol mol}^{-1}$ .

Volatiles in the chamber air were collected onto multibed stainless steel cartridges (10.5 cm length, 4 mm inner diameter; Supelco, Bellefonte, PA, USA) using a constant flow air sample pump (210-1003MTX; SKC Inc., Houston, TX, USA) operated at a rate of 200 ml min<sup>-1</sup> for 20 min, resulting in quantitative adsorption of volatiles from 4 liters of air. The cartridges were filled with Carbotrap C 20/40 mesh (0.2 g), Carbopack B 40/60 mesh (0.1 g), and Carbotrap X 20/40 (0.1 g) adsorbents (Supelco) for optimal adsorption of volatiles in the C5–C15 range (Kännaste *et al.*, 2014). Before the collection of volatiles, the traps were cleaned by passage of a stream of ultra pure helium at a flow rate of 200 ml min<sup>-1</sup> at 400 °C for 2 h using a SIM Clean-Cube cartridge thermo-conditioner (Scientific Instruments Manufacturer GmbH, Oberhausen, Germany). After each treatment, the chamber and tubing were flushed with a stream of ozone (~1000 ppm) to eliminate the volatiles adsorbed by the chamber and tubes that could contaminate the measurement system (mainly MeJA, and to a low degree stress-induced volatiles; Niinemets *et al.* 2011).

The volatile samples were collected before leaf treatment with MeJA and 20 min, 2, 10, and 24 h after treatment with MeJA. Blank empty chamber measurements were taken before and after the experiment. During and after the experiment, additional blank samples were taken from the adjacent empty chamber operated under identical conditions, and the baseline during the experiment was adjusted when needed using the blanks from the experimental chamber and empty chamber at the end of the experiment (the difference between the two blanks was small, indicating that the system memory effect was minor). After 36–48 h, the experiment was finished, and the treated leaf was removed, scanned, and its area was estimated with the UTHSCSA ImageTool 2.0 (Dental Diagnostic



Science, The University of Texas Health Science Center, San Antonio, TX, USA). These leaf images were further used to assess the quantitative degree of damage (Fig. 1A).

#### Gas-chromatographic analysis of volatiles

Adsorbent cartridges were analyzed according to the method of Kännaste *et al.* (2014) using a combined Shimadzu TD20 automated cartridge desorber and a Shimadzu 2010 Plus gas chromatograph with mass spectrometric detector (GC-MS; Shimadzu Corporation, Kyoto, Japan). A C8–C20 hydrocarbon standard (Sigma-Aldrich) was used to obtain the retention indices as in Pazouki *et al.* (2015) and in Jiang *et al.* (2016b) (Table 2). Compounds were identified using the NIST spectral library, the spectral and retention indices library of Adams (1995), and a custom-made library of retention times and mass spectra of commercially available mono- and sesquiterpene standards (GC purity, Sigma-Aldrich). The authentic standards were also used for GC-MS calibration as described in detail in Kännaste *et al.* (2014). The background (blank) concentrations of individual volatiles in the empty chamber were subtracted from the plant samples, and the emission rates were calculated according to the equations of Niinemets *et al.* (2011).

#### Online monitoring of the kinetics of volatile release

A high-resolution PTR-TOF-MS (TOF8000, Ionicon Analytik, Innsbruck, Austria) was used to track the volatile release in real time. The PTR-TOF-MS system was connected to a custom-designed two-channel gas-exchange system described in detail by Copolovici

and Niinemets (2010). The measurement cuvette (1.2 l) consisted of a stainless steel bottom and a double-walled glass upper part specially designed for volatile compound measurements. A thermostat was used to control the temperature of water circulating between the glass chamber walls, and the chamber air temperature was within  $\pm 0.2$  °C of the chamber wall temperature. Four wide-beam halogen lamps (Osram GmbH, Germany) were used for chamber illumination. Ambient air that was purified through the passage of a charcoal filter and an ozone trap, and humidified to the desired water vapor pressure was used (Copolovici and Niinemets, 2010). The flow rate through the system was  $1.6 \text{ l min}^{-1}$ , and the sample air was drawn into the PTR-TOF-MS drift tube at a flow rate of  $100 \text{ ml min}^{-1}$ . Background volatile concentrations in the ambient air pumped into the chamber were assessed in the reference mode, and volatile concentrations in the outgoing air stream were measured in the sample mode. In addition, measurements with the empty chamber were also conducted before and after plant measurements. In these experiments, chamber temperature was maintained at 25 °C, light intensity at the leaf surface at  $500 \mu\text{mol m}^{-2} \text{ s}^{-1}$ , chamber air humidity between 50% and 60% (vapor pressure deficit of 1.2–1.6 kPa), and  $\text{CO}_2$  concentration between  $370 \mu\text{mol mol}^{-1}$  and  $400 \mu\text{mol mol}^{-1}$ . After enclosure of the MeJA-treated leaf, all measurements were immediately started.

The operation of the PTR-TOF-MS, system calibration, and compound detection followed the protocol of Portillo-Estrada *et al.* (2015). In brief, the drift tube conditions were 2.3 mbar, 600 V, and 60 °C, the measurements were carried out continuously through the mass to charge ratio ( $m/z$ ) range of 0–316, and data for 31 250 spectra  $\text{s}^{-1}$  were averaged. The raw PTR-TOF-MS data were post-processed with the PTR-MS Viewer 3.0.0.99 (ToFwerk AG, Switzerland), and relevant  $m/z$  peaks were integrated as explained in Portillo-Estrada *et al.* (2015). The time resolution used in this study is 10 s (the averaged data were recorded every 10 s). Methanol was detected as the protonated parent ion with an  $m/z$  of 33, while the total emission of volatiles produced within the octadecanoid pathway (LOX products) was taken as the sum of individual ion masses ( $m/z$ ) of 57 [ $m_{57}$ , (*E*)-2-hexenal (frag)], 81 [ $m_{81}$ , (*Z*)-3-hexenal+(*E*)-3-hexenal (frag)] after correction for the share of the fraction originating from monoterpenes; see below, 83 [ $m_{83}$ , hexenol+hexenal (frag)], 85 [ $m_{85}$ , hexenol (frag)], 103 [ $m_{103}$ , hexenol (main)], 99 [ $m_{99}$ , (*Z*)-3-hexenal+(*E*)-3-hexenal (main)], and 101 [ $m_{101}$ , (*Z*)-3-hexenal+(*E*)-3-hexenol+(*E*)-2-hexenol+hexenal (main)] (Copolovici and Niinemets, 2010; Portillo-Estrada *et al.*, 2015). Total monoterpene emission was characterized by the parent ion with an  $m/z$  of 137 ( $m_{137}$ ), and total sesquiterpene emission by the parent ion with  $m/z$  205 ( $m_{205}$ ). As even under the soft ionization conditions of the operation of PTR-TOF-MS used here, monoterpenes can partly fragment, with the fragment spectrum dominated by the mass fragments with  $m/z$  67, 81, and 95 (Copolovici *et al.*, 2005; Tani *et al.*, 2003), use of parent ions somewhat underestimates the emissions of monoterpenes. Based on simultaneous GC-MS measurements, for total monoterpenes, we divided the concentration of the parent ion by  $m/z$  137 by 0.46 to obtain total monoterpene emission. To consider the interference of the mass fragment with  $m/z$  81 coming from monoterpene fragmentation with the detection of the LOX compound 3-hexenal, fragmentation of which also produces the identical mass fragment, we separately analyzed the PTR-TOF-MS fragmentation spectra of (*Z*)-3-hexenal and all emitted terpenoids, and developed appropriate equations to assess the share of  $m/z$  81 from monoterpenes and 3-hexenal based on the concentration of corresponding parent ions.

The emission rates per unit leaf area were calculated according to Niinemets *et al.* (2011) considering both the incoming air measurements taken frequently during the experiments and empty chamber measurements before plant enclosure (typically only differing slightly from the incoming air concentrations). PTR-TOF-MS measurements were continued until the elicited emissions reached the background level, usually between 36 h and 48 h after the treatment (Fig. 2).

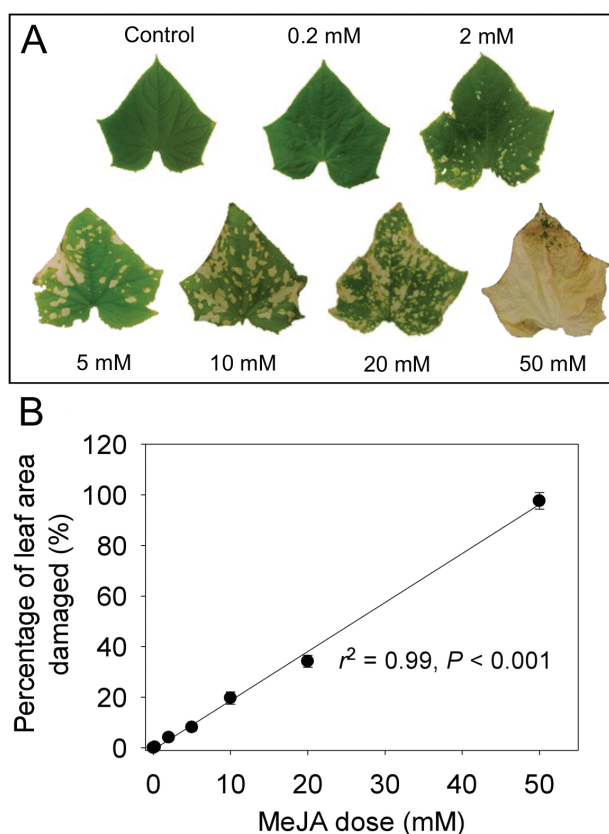


**Fig. 1.** Characteristic images of MeJA-treated cucumber (*Cucumis sativus*) leaves taken 36–48 h after treatment with MeJA concentrations of 0 (control), 0.2, 2, 5, 10, 20, and 50 mM (A), and corresponding relationship between the percentage of damage and applied MeJA concentration (B). The data in (B) were fitted by a linear regression ( $y = 1.94x - 0.71$ ;  $r^2 = 0.99$ ,  $P < 0.001$ ).

### Quantitative characterization of elicitation of volatile emissions by MeJA treatment

Time-courses of emissions induced by MeJA treatment were either biphasic with two maxima (LOX products; Fig. 2A, B) or monophasic (monoterpenes, sesquiterpenes, and methanol; Fig. 2C, D). The emission time-courses were used to derive the key quantitative emission characteristics (Fig. 2; Table 1), including the emission rates at the two emission maxima ( $\Phi_{M1}$  and  $\Phi_{M2}$ ), the corresponding times for the emission maxima ( $t_{M1}$  and  $t_{M2}$ ), the durations of the two emission peaks ( $D_{P1}$  and  $D_{P2}$ ), the duration between the emission maxima ( $D_M$ ), and the total volatile emissions corresponding to both emission bursts ( $I_{T1}$  and  $I_{T2}$ ). For the first emission burst, the total integrated emission was calculated as:

$$I_{T1} = \int_{t_{P1S}}^{t_{P1E}} \Phi(t) dt, \quad (1)$$

where  $\Phi(t)$  is the emission rate at time  $t$ ,  $t_{P1S}$  is the start, and  $t_{P1E}$  is the end of the first induced emission release. In practice, numerical integration according to the trapezoidal rule was used and the infinitesimal time period  $dt$  was replaced by the measurement period  $\Delta t$  of 10 s. The integrated emission corresponding to the second emission burst was calculated analogously.

The emission kinetics of different volatiles followed a similar pattern characterized by an initial exponential increase, then by slowing down of the rate of increase until the emissions reached the maximum value, followed by a non-linear decay to the baseline emission (Fig. 2). We fitted the initial parts of the increase and decay of the emissions corresponding to the first and the second emission burst with simple first-order exponential models. For the first peak,

$$\Phi(t) = \Phi(t_{P1S})e^{k_{I1}t}, \quad (2)$$

for the increasing part, and

$$\Phi(t) = \Phi(t_{M1})e^{-k_{D1}t}, \quad (3)$$

for the decreasing part. Here,  $k_{I1}$  is the rate constant for the increase and  $k_{D1}$  is the rate constant for the decrease of emission of the given compound. If present, the rate constants for the increase and decrease for the second peak ( $k_{I2}$  and  $k_{D2}$ ) were calculated analogously. From the rate constants, corresponding doubling times [e.g. for the first emission burst,  $\tau_{I1} = \ln(2)/k_{I1}$ ] and decay half-times [ $\tau_{D1} = \ln(2)/k_{D1}$ ] for both emissions bursts were also calculated.

### Data analyses

All experiments were replicated three times with different plants, and all data shown are averages  $\pm$ SE. Effects of MeJA dose were studied by linear or non-linear regressions depending on the shape of the response. Emission rates of volatiles elicited by different MeJA concentrations at fixed time points estimated by GC-MS were compared by ANOVA followed by post-hoc Tukey's test. The analyses were conducted with SAS (Version 8.02; SAS Institute, Cary, NC, USA) and all statistical effects are considered significant at  $P < 0.05$ .

## Results

### Methyl jasmonate treatments in leaves of *Cucumis sativus*: general patterns and short- and long-term emission responses

Control plants were weak emitters of monoterpenes  $\alpha$ -pinene, camphene,  $\beta$ -pinene, and  $\Delta^3$ -carene, several longer aliphatic

aldehydes C7–C10, some characteristic C6 lipoxygenase pathway volatiles (LOX), and benzaldehyde (Table 2). MeJA treatment resulted in rapid elevation of C6 and derivative LOX products, (Z)-3-hexen-1-ol, 3-hexenyl acetate, (Z)-3-hexen-1-ol, and *n*-hexanal, detectable with GC-MS already at 20 min after treatment. Moreover, 6-methyl-5-hepten-2-one and heptanal could also be induced significantly by higher concentrations of MeJA (10 mM and 20 mM). Emissions of C6-LOX compounds in the treated plants were strongly reduced at the second sampling event at 2 h, and the emissions increased again at 10 h, especially C6-LOX compounds and derivatives (Table 2). However, 3-hexenyl acetate was not detectable in any of the MeJA dose treatments after the initial elevation at 20 min. In 24 h after the treatment, (Z)-3-hexen-1-ol could not be identified in any of the MeJA dose treatments, and the emission rate of *n*-hexanal decreased dramatically compared with the emission rate at 10 h. However, nonanal and decanal emissions remained at a moderately high level throughout the treatments (Table 2).

In contrast to aliphatic aldehydes and LOX, no enhancement of monoterpene emissions and no sesquiterpene emissions in MeJA-treated leaves were observed at the first two measurement events (Table 2). However, monoterpene emissions, especially limonene and  $\Delta^3$ -carene emissions, were enhanced in MeJA-treated leaves at 10 h and, at this sampling event, emissions of the monoterpene linalool, and sesquiterpenes  $\beta$ -farnesene,  $\alpha$ -cedrene, and  $\beta$ -caryophyllene were identified (Table 2). At 24 h after the treatment, terpenoid emissions had mostly reached the pre-treatment level (Table 2).

In 36–48 h after the exposure to MeJA, all treated leaves except those from the 0.2 mM treatment exhibited a certain degree of damage ranging from chlorotic spots in the 2 mM treatment to major chlorotic areas in 5–20 mM treatments, and at the lethal concentration of 50 mM, the damage was spread over the entire leaf area (Fig. 1A). The damaged leaf area was linearly correlated with the concentration of MeJA applied (Fig. 1B).

High time resolution measurements of kinetics of elicitation of volatile emissions in MeJA-treated leaves by PTR-TOF-MS broadly confirmed the timing of release of different compounds highlighted by GC-MS analyses (Fig. 2). PTR-TOF-MS measurements also confirmed the occurrence of two emission bursts for LOX, a fast burst elicited immediately after MeJA treatment and reaching a maximum in  $\sim 0.2$ –1 h, and a slower burst elicited in 6–10 h after MeJA treatment and reaching a maximum in  $\sim 16$ –20 h (Fig. 2A, B). In the case of mono- ( $m/z$  137) and sesquiterpenes ( $m/z$  205), only one slower burst was observed (Fig. 2C). This slower burst started in 2–6 h after MeJA treatment and reached a maximum in  $\sim 15$ –25 h (Fig. 2C). Apart from the compounds detected by GC-MS, PTR-TOF-MS measurements demonstrated a major burst of methanol emission (Fig. 2D). Methanol ( $m/z$  33) emissions started almost immediately after MeJA treatment, and reached a maximum  $\sim 0.5$ –1.5 h after the treatment (Fig. 2D).

The MeJA threshold concentration for elicitation of both the rapid and the slow LOX emission bursts and the methanol

**Table 2.** Average ( $\pm$  SE) emission rates ( $\text{pmol m}^{-2} \text{s}^{-1}$ ) of individual volatile compounds after treatment of MeJA with different doses over the time-course of 24 h identified by GC-MS

Volatile Compounds	Retention index	20 min					2 h				
		Control	2 mM	5 mM	10 mM	20 mM	Control	2 mM	5 mM	10 mM	20 mM
Lipoxygenase pathway products and saturated aldehydes											
(E)-3-Hexenal	802	120 ± 24a	167 ± 37a	608 ± 87ab	663 ± 87ab	860 ± 140b	80 ± 17	71 ± 11	110 ± 24	180 ± 24	130 ± 20
(Z)-3-Hexen-1-ol	863	ND <sup>a</sup>	ND	130 ± 17a	342 ± 68ab	1000 ± 140b	ND	ND	4.7 ± 1.9	5.7 ± 0.7	10.1 ± 2.4
Heptanal	899	ND	ND	101 ± 18	182 ± 39	152 ± 22	ND	ND	ND	115 ± 12	76 ± 17
Octanal	1074	105 ± 19	183 ± 32	110 ± 17	201 ± 30	161 ± 21	177 ± 24	223 ± 22	94 ± 22	219 ± 16	167 ± 24
(Z)-3-Hexen-1-yl acetate	1008	ND	ND	2160 ± 290	1930 ± 210	3270 ± 810	ND	ND	ND	ND	ND
2-Ethyl-1-hexanol	1046	130 ± 31	229 ± 63	137 ± 18	249 ± 37	201 ± 28	222 ± 27	278 ± 32	118 ± 22	273 ± 29	208 ± 27
Nonanal	1098	502 ± 74	868 ± 99	521 ± 99	950 ± 170	763 ± 124	843 ± 112	1050 ± 140	446 ± 81	1042 ± 81	790 ± 140
Decanal	1204	561 ± 99	977 ± 81	590 ± 120	1060 ± 150	857 ± 112	945 ± 87	1180 ± 170	505 ± 93	1166 ± 93	890 ± 120
Monoterpenes											
α-Pinene	932	76 ± 11	50 ± 11	81 ± 12	62.6 ± 9.9	86.2 ± 9.9	78 ± 11	57.0 ± 7.4	41.5 ± 9.3	58.9 ± 8.1	65.7 ± 8.7
Camphene	949	1.4 ± 0.4	1.4 ± 0.6	1.0 ± 0.4	2.0 ± 0.3	2.4 ± 0.6	1.9 ± 0.3	1.9 ± 0.5	1.4 ± 0.3	3.6 ± 0.6	2.9 ± 0.4
β-Pinene	980	3.3 ± 1.0	4.3 ± 1.2	3.6 ± 0.7	2.9 ± 0.6	3.3 ± 1.0	2.2 ± 0.6	3.5 ± 0.9	4.7 ± 1.1	6.4 ± 0.9	6.1 ± 0.9
Δ <sup>3</sup> -Carene	1011	36.6 ± 8.9	31.6 ± 8.7	55.8 ± 9.9	65.7 ± 8.7	71 ± 19	39.1 ± 5.6	64.5 ± 7.4	31.4 ± 5.6	26.0 ± 6.2	55.2 ± 6.8
Limonene	1029	ND	ND	ND	ND	ND	ND	ND	ND	ND	ND
Linalool	1098	ND	ND	ND	ND	ND	ND	ND	ND	ND	ND
Sesquiterpenes											
α-Cedrene	1409	ND	ND	ND	ND	ND	ND	ND	ND	ND	ND
β-Caryophyllene	1428	ND	ND	ND	ND	ND	ND	ND	ND	ND	ND
β-Farnesene	1455	ND	ND	ND	ND	ND	ND	ND	ND	ND	ND
Geranylgeranyl diphosphate (GGDP) pathway derived volatiles <sup>b</sup>											
6-Methyl-5-hepten-2-one	985	158 ± 29a	366 ± 56ab	185.4 ± 29a	513 ± 58ab	1810 ± 320b	99 ± 17a	252 ± 32ab	231 ± 56ab	455 ± 56ab	1100 ± 170b
Geranylacetone	1453	34.2 ± 1.4	59 ± 13	36.0 ± 5.6	65 ± 11	52.1 ± 5.0	57.7 ± 6.2	73 ± 12	31.4 ± 9.3	71.3 ± 8.1	53.9 ± 8.7
Benzenoids											
Benzaldehyde	967	180 ± 37a	126 ± 19a	236 ± 62a	550 ± 87ab	890 ± 110b	148 ± 18	158 ± 22	167 ± 37	107.9 ± 7.4	137 ± 19

Three replicate treatments at each MeJA application concentration were carried out. Means among treatments and sampling times were compared by ANOVA followed by post-hoc Tukey's tests, and statistically significant differences are denoted by different lowercase letters. For compounds without labels, the emission rates did not differ significantly among treatments at different sampling events.

The pathways leading to saturated aliphatic aldehydes are not yet fully resolved, although these emissions are also up-regulated upon abiotic and biotic stresses similarly to lipoxygenase volatiles (Wildt et al., 2003; Hu et al., 2009).

The data of the 50 mM treatment are not shown in the table because this lethal dose caused a rapid necrosis in 1 h and no volatile emission was detected then from the leaves, implying the loss of the biological activity.

<sup>a</sup> ND, below the detection limit of  $\sim 0.1 \text{ pmol m}^{-2} \text{s}^{-1}$ .

<sup>b</sup> Carotenoid breakdown products including geranyl acetone (Gao et al., 2008; Arimura et al., 2009; Kask et al., 2016).

emission burst was 2 mM, while for monoterpenes the threshold concentration was 0.2 mM and for sesquiterpenes 2 mM. The slower emission burst for LOX and the emission bursts for monoterpenes and sesquiterpenes were absent for leaves treated with the highest (lethal, Fig. 1A) MeJA concentration of 50 mM.

#### MeJA elicits volatile emissions in a dose-dependent manner

The maximum emission rate of MeJA-elicited emissions increased with increasing MeJA concentration for both the faster (Fig. 3A, B) and the slower (Fig. 3A, C, D) MeJA response. The dependencies of the maximum emission rates of volatiles on MeJA concentration were somewhat non-linear, implying that the increases of the maximum emission rates were greater at greater MeJA treatment

concentration, especially between the concentrations of 10 mM and 20 mM and 20 mM and 50 mM (Fig. 4). The emission maxima scaled positively with the degree of leaf damage (insets in Fig. 3). MeJA dose dependencies of emission rates of LOX in the early response phase and of LOX and mono- and sesquiterpenes in the late phase were also evident in GC-MS data. However, due to the lower time resolution, the variability in these responses was greater (Table 2).

The total integral emissions (Equation 1; Fig. 2 for definition) also scaled positively with the MeJA treatment concentration for both the faster (Fig. 4A, B) and the slower (Fig. 4A, C, D) emission responses. However, although the emission maxima at a given MeJA concentration were similar for the first and the second emission bursts of LOX compounds (Fig. 3A), the total LOX emission corresponding to the second emission burst was much larger than that for

10 h					24 h				
Control	2 mM	5 mM	10 mM	20 mM	Control	2 mM	5 mM	10 mM	20 mM
76 ± 20a	46.5 ± 6.8a	298 ± 62ab	820 ± 130b	720 ± 150b	63 ± 14	81 ± 12	123 ± 14	161 ± 22	169 ± 19
ND	18.9 ± 2.1a	64 ± 12ab	304 ± 43b	252 ± 23b	ND	ND	ND	ND	ND
ND	ND	102 ± 11	223 ± 37	233 ± 29	ND	ND	20.2 ± 3.3	27.9 ± 3.0	21.3 ± 1.9
101 ± 17	131 ± 18	167 ± 24	42.8 ± 9.9	98 ± 16	66 ± 14	137 ± 17	144 ± 15	109 ± 18	140 ± 19
ND	ND	ND	ND	ND	ND	ND	ND	ND	ND
127 ± 19	163 ± 23	208 ± 26	53.9 ± 9.3	122 ± 23	83 ± 16	172 ± 11	180 ± 17	136 ± 23	176 ± 24
484 ± 87	620 ± 110	794 ± 93	204 ± 29	465 ± 99	316 ± 63	650 ± 120	682 ± 99	515 ± 87	660 ± 120
542 ± 74	699 ± 81	888 ± 81	229 ± 31	523 ± 94	353 ± 62	731 ± 93	769 ± 87	580 ± 93	750 ± 81
64.5 ± 9.3	100 ± 11	99.2 ± 9.3	182 ± 38	246 ± 34	107 ± 14	52.7 ± 7.4	39.1 ± 4.3	36.0 ± 5.6	35.3 ± 4.3
2.2 ± 0.4	3.0 ± 0.3	5.1 ± 0.9	9.9 ± 2.1	15.5 ± 4.3	0.62 ± 0.09a	2.0 ± 0.4ab	3.41 ± 0.682b	6.51 ± 0.87bc	8.7 ± 1.1c
2.6 ± 0.4	2.9 ± 0.6	5.8 ± 1.1	5.8 ± 1.8	8.1 ± 1.6	0.66 ± 0.06	2.2 ± 0.4	1.8 ± 0.3	3.2 ± 0.6	2.9 ± 0.4
43.4 ± 5.0a	55.8 ± 8.7a	133 ± 19b	311 ± 50bc	477.4 ± 68c	53.3 ± 8.1	40.3 ± 6.2	29.1 ± 3.1	67.6 ± 8.1	57.0 ± 9.3
ND	ND	254 ± 37	428 ± 50	378 ± 50	ND	ND	42.0 ± 8.6	43.2 ± 8.4	99 ± 25
ND	ND	7.0 ± 1.0	22.2 ± 2.5	18.0 ± 3.7	ND	ND	ND	ND	ND
ND	ND	ND	18.3 ± 3.0	30.4 ± 4.3	ND	ND	ND	9.3 ± 3.1	ND
ND	ND	ND	4.6 ± 1.1	9.4 ± 2.2	ND	ND	ND	ND	ND
ND	7.1 ± 1.9	4.8 ± 0.7	8.7 ± 2.2	13.4 ± 3.0	ND	ND	ND	0.7 ± 0.3	ND
152 ± 19	179 ± 25	145 ± 19	199 ± 32	114 ± 12	15.2 ± 2.8	17.9 ± 2.8	214.5 ± 2.5	19.9 ± 2.2	70.1 ± 6.8
32.9 ± 7.4	42.2 ± 9.3	53.9 ± 7.4	14.0 ± 2.5	31.6 ± 5.0	21.5 ± 2.5	44.6 ± 8.7	46.5 ± 8.7	35.3 ± 3.1	45.9 ± 5.0
32.9 ± 7.4a	118 ± 12a	210 ± 25ab	515 ± 74ab	869 ± 99b	484 ± 87	205 ± 22	156 ± 19	113 ± 16	68.8 ± 4.3

the first emission burst (Fig. 4A), and thus the total release of LOX compounds during the whole experiment mainly scaled with the slower LOX response (Fig. 4A). Stronger elicitation of the slower emission response was particularly evident for lower concentrations of MeJA such that the ratio of the second ( $I_{T,LOX2}$ ) to the first ( $I_{T,LOX1}$ ) integrated emission scaled negatively with MeJA concentration (Fig. 5A).

For total integrated emission versus MeJA concentration relationships, the non-linearity was much less than for maximum emission versus MeJA relationships (cf. Figs 3 and 4). In fact, the total LOX emissions corresponding to both the first and the second emission bursts were best fitted by linear regressions (Fig. 4A). Analogously with the maximum emissions, total LOX emissions were strongly correlated with the degree of leaf damage through the MeJA treatments (insets in Fig. 4).

#### *Timing and rate of elicitation of volatile emissions depend on MeJA concentration*

MeJA concentration significantly affected the timing of volatile emission responses. The maxima for both the faster and the slower LOX emission bursts occurred earlier at higher MeJA concentration, whereas the change in the timing was greater for the faster LOX burst (Fig. 5B). In contrast, the maximum emission for the methanol burst occurred later at a greater MeJA concentration (Fig. 5C). Similarly to LOX, the maxima of monoterpene and sesquiterpene emissions also occurred earlier at higher MeJA concentrations, and this concentration response was stronger for monoterpenes (Fig. 5D).

To characterize further the MeJA effects on the emission kinetics, the induction ( $k_1$ , Equation 2) and decay ( $k_D$ , Equations 2 and 3) rate constants (see also Table 1) were determined. This analysis indicated that both the initial increase



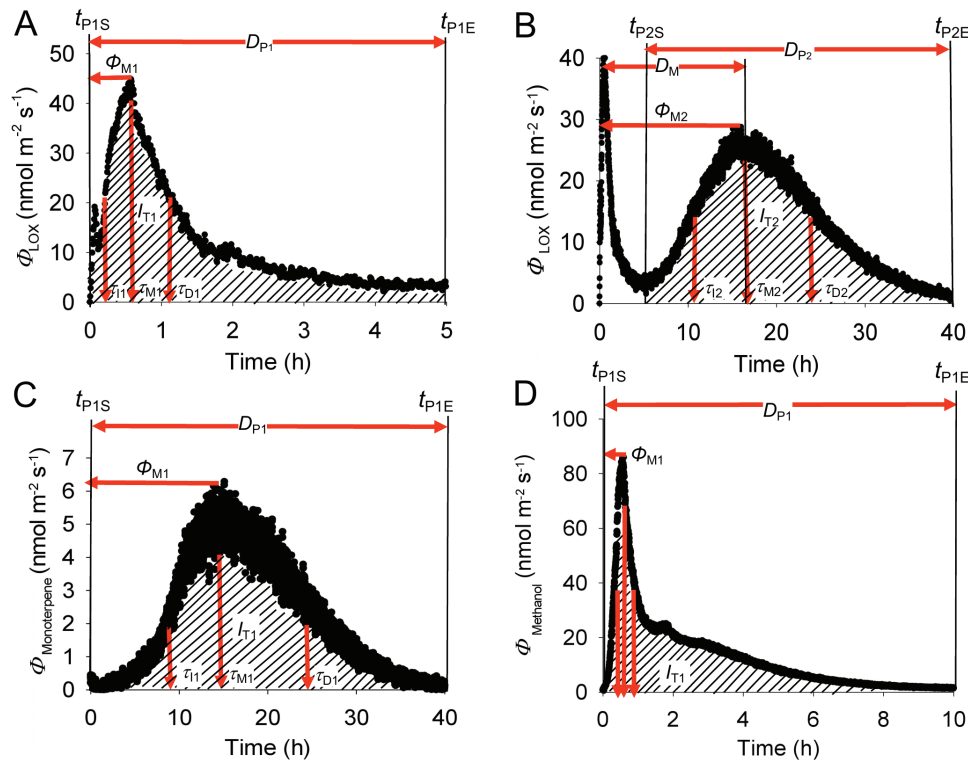


**Fig. 2.** Representative time-courses of methyl jasmonate (MeJA)-induced emissions from a *C. sativus* leaf, and definition of key variables characterizing the induction response (see Table 1 for further specifics). Volatile emissions were induced by application of 20 mM MeJA that elicited an early lipoxygenase pathway volatile (LOX) burst (A), and a second late LOX emission burst (B) with concomitant monoterpene emission burst (C) and an early slowly decaying methanol emission burst (D). Shaded areas in all panels indicate integrated emissions corresponding to individual emission bursts ( $I_{T1}$  for the first and  $I_{T2}$  for the second burst, Equation 1),  $\Phi_{T1}$  and  $\Phi_{T2}$  correspond to the emission maxima for the two bursts, and  $t_{M1}$  and  $t_{M2}$  denote the corresponding times from the start of the treatment. Different  $\tau$ -s stand for the initial doubling and decay times for the two bursts (Table 1). In (D), the red vertical arrows show the positions of  $\tau_{T1}$ ,  $t_{M1}$ , and  $\tau_{D1}$  as in the other panels. After the leaf treatment with MeJA, the release of emissions was continuously monitored with a proton-transfer reaction time-of-flight mass spectrometer (PTR-TOF-MS). The time kinetics of sesquiterpene emission is analogous to monoterpene emissions and is therefore not presented.

and decrease of emissions was faster at higher MeJA concentrations for LOX compounds (Fig. 6A, B) and terpenoids (Fig. 7A, B). However, for methanol, the rate constants  $k_1$  and  $k_D$  initially decreased over the MeJA concentration range of 0.2–5 mM, and they were weakly affected by MeJA concentrations >5 mM (Fig. 6C). Both the rise and decline kinetics were much faster for the first than for the second LOX emission burst (Fig. 6A, B). In addition, MeJA concentration dependencies of  $k_1$  and  $k_D$  were weaker for the second LOX emission burst, with a moderate change in the induction and decay rates over the MeJA concentration range of 5–20 mM (Fig. 6A, B). The induction and decay rates were similar for mono- and sesquiterpenes, except for the lowest MeJA treatment concentration of 0.2 mM that barely induced sesquiterpene release (Fig. 6C, D).

Despite a faster rate of decline at greater MeJA concentrations, induction to a higher maximum level at greater MeJA concentration (Fig. 3) implied that the total length of the emission burst increased with increasing MeJA concentration for all compound classes (Figs 6D, 7C), except for the first LOX burst (Fig. 6D). In the case of the early LOX release, the duration of the pulse length decreased between 2mM and 5 mM MeJA, and was thereafter invariable (Fig. 6D).

## Discussion

### Exposure to MeJA leads to rapid bursts of characteristic stress volatiles in *Cucumis sativus*

A variety of biotic stresses elicits emissions of volatile products of the lipoxygenase pathway (LOX compounds, also called green leaf volatiles) (Matsui et al., 2012; Scala et al., 2013). LOX compounds are synthesized by multiple lipoxygenases and fatty acid hydroperoxide lyases, several of which are constitutively active in leaves (Feussner and Wasternack, 2002), implying that as soon as the substrates, polyunsaturated fatty acids, are released from membranes, LOX products are rapidly emitted. Typically, the early LOX response occurs within 2–30 min after biotic stress treatment (Zhang and Xing, 2008; Bruinsma et al., 2009; Brilli et al., 2011; War et al., 2012; Portillo-Estrada et al., 2015), and this rapid LOX burst has been shown to be involved in priming and triggering subsequent local and systemic stress responses (Farag and Paré, 2002; Mithöfer et al., 2005; Niinemets et al., 2013; Scala et al., 2013).

In our study, LOX emissions were detected immediately after enclosure of treated leaves in the measurement system, and the emissions reached the first maximum in 0.1–1 h depending on MeJA concentration (Figs 2A, 5B). The increase was faster than the decrease (cf. Fig. 6A, B).



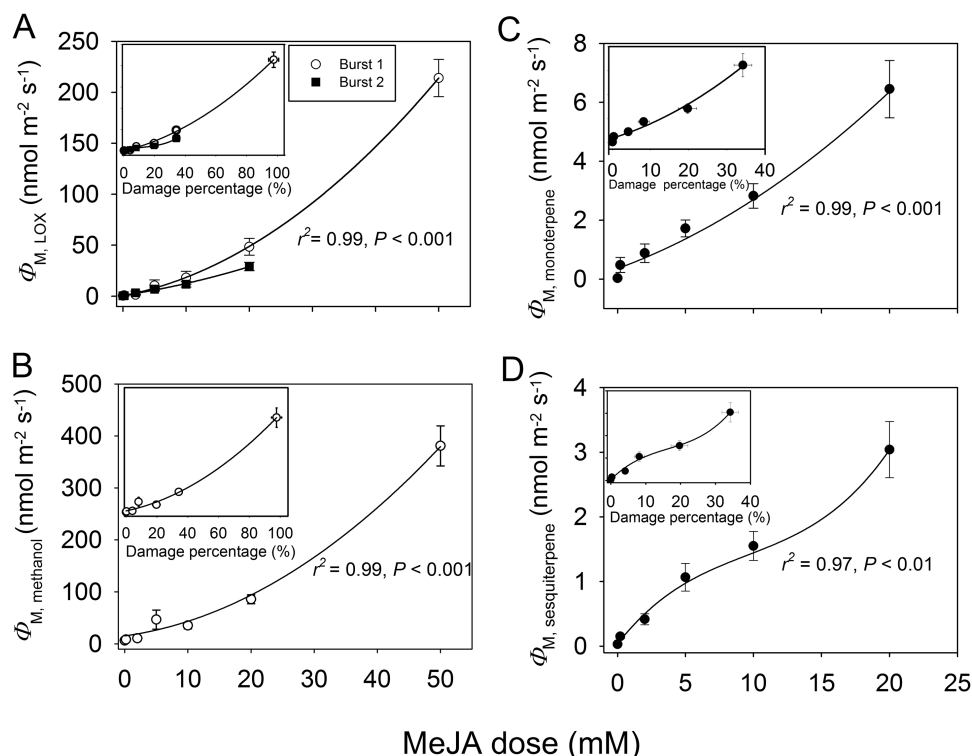


**Fig. 3.** Maximum emission rates of LOX ( $\Phi_{M, LOX}$ , A), methanol ( $\Phi_{M, methanol}$ , B), monoterpenes ( $\Phi_{M, monoterpene}$ , C), and sesquiterpenes ( $\Phi_{M, sesquiterpene}$ , D) as dependent on the applied MeJA dose and corresponding correlations with the degree of damage at the end of the experiment (insets) in leaves of *C. sativus* (see Fig. 2 for sample-induced emission kinetics). MeJA treatments as in Fig. 1. Treatment with 50 mM MeJA was lethal (Fig. 1) and, thus, the second LOX emission burst and monoterpene and sesquiterpene emission bursts were absent at this concentration. Data were fitted by second-order polynomial regressions, except that sigmoidal regressions were used for (D). For the first LOX burst in (A),  $y = 0.062x^2 + 1.19x + 0.46$  (main panel) and  $y = 0.013x^2 + 0.89x - 0.3$  (inset). For the second LOX burst in (A),  $y = 0.0335x^2 + 0.94x + 0.46$  (main panel) and  $y = 0.013x^2 + 0.37x + 1.05$  (inset). For methanol in (B),  $y = 0.11x^2 + 1.65x + 12.0$  (main) and  $y = 0.026x^2 + 1.28x + 10.9$  (inset), for monoterpenes in (C),  $y = 0.0037x^2 + 0.23x + 0.30$  (main) and  $y = 0.0023x^2 + 0.098x + 0.36$  (inset), and for sesquiterpenes in (D),  $y = 3.26/[1 + e^{(9.80 - x)/4.02}]$  (main) and  $y = 3.72/[1 + e^{(21.5 - x)/8.72}]$  (inset). For the relationships in (A–C),  $r^2 = 0.99, P < 0.001$ , except for the second LOX burst versus damage percentage in (A) where  $r^2 = 0.98, P < 0.01$ . In (D),  $r^2 = 0.97, P < 0.01$  for the main panel and  $r^2 = 0.96, P < 0.01$  for the inset. Three replicate treatments at each MeJA application concentration were carried out.

such that the emissions corresponding to this initial burst were maintained at a moderately high level for several hours after the MeJA treatment (Fig. 2A). Thus, this early MeJA response clearly reflects activation of constitutive lipoxygenases (LOX), hydroperoxide lyase (HPL), allene oxide synthase (AOS), and alcohol dehydrogenase (ADH), resembling the rapid response to wounding herbivores (Brilli *et al.*, 2011; Portillo-Estrada *et al.*, 2015).

Concomitant with the start of LOX emissions, major methanol emissions were elicited (Fig. 2D). Release of methanol is a characteristic stress response that reflects activation of demethylation of cell wall pectins by constitutively expressed pectin methylesterases (Micheli, 2001; Pelloux *et al.*, 2007). Previous studies have demonstrated activation of methanol release upon leaf mechanical wounding (Brilli *et al.*, 2011; Portillo-Estrada *et al.*, 2015), insect feeding (Peñuelas *et al.*, 2005; von Dahl *et al.*, 2006), fungal infestation (Copolovici *et al.*, 2014b; Jiang *et al.*, 2016b), and ozone exposure (Beauchamp *et al.*, 2005). Such cell wall modifications can importantly enhance the penetration of downstream signaling compounds (Gális *et al.*, 2009), including MeJA diffusion. Furthermore, there is evidence that in addition to LOX volatiles, methanol is not only the by-product of stress-dependent

cell wall modifications, but also can serve as an important signal eliciting or modifying systemic stress responses (von Dahl *et al.*, 2006; Seco *et al.*, 2011; Hann *et al.*, 2014; Komarova *et al.*, 2014).

#### *Biphasic MeJA elicitation of volatile emissions in C. sativus*

The fast emission burst of LOX and methanol was followed by slower emission bursts of LOX (Fig. 2B), monoterpenes (Fig. 2C), and sesquiterpenes that reached a maximum in 16–25 h after MeJA treatment (Fig. 5B, C). Constitutive monoterpene emissions are very low in non-stressed cucumber (Table 2), and the emissions were not significantly elicited by MeJA over the short term, suggesting that the longer term elicitation of terpenoid emissions reflects a gene expression level response as has been observed in several studies looking at MeJA-dependent stress responses (Martin *et al.*, 2002, 2003; Byun-McKay *et al.*, 2006). Furthermore, the induced monoterpene blend significantly differed from the blend of constitutive emissions (Table 2), further supporting the argument that the induced monoterpene emissions reflected expression of

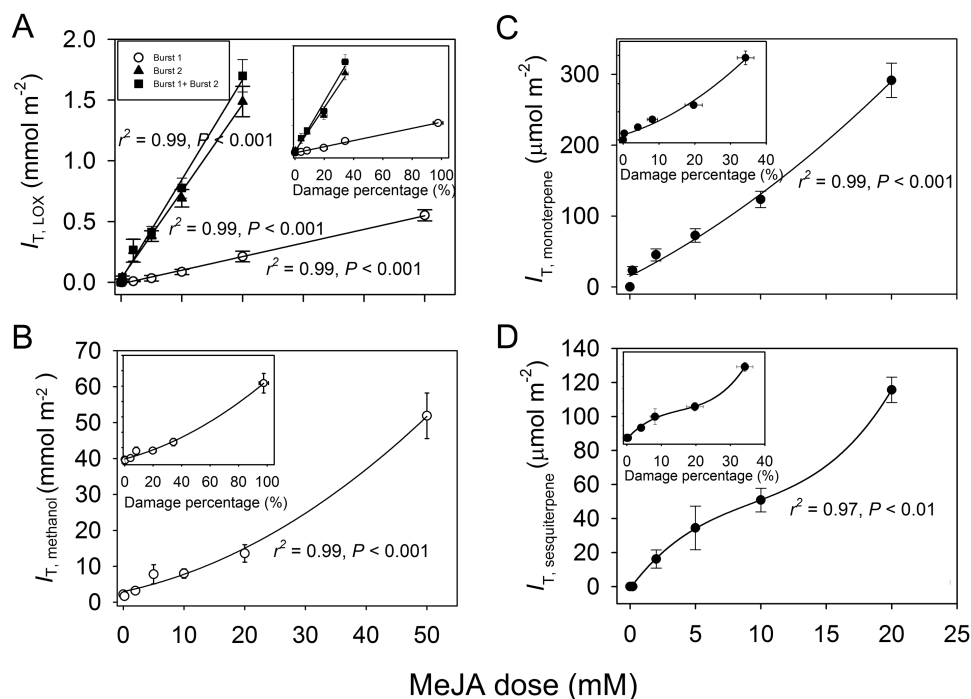


**Fig. 4.** Integrated emissions ( $I_T$ , Equation 1) of lipoxigenase pathway volatiles ( $I_{T, LOX}$ , A), methanol ( $I_{T, methanol}$ , B), monoterpenes ( $I_{T, monoterpene}$ , C), and sesquiterpenes ( $I_{T, sesquiterpene}$ , D) in relation to the applied MeJA concentration and corresponding relationships with the degree of damage (insets) in leaves of *C. sativus* (see Fig. 2 for the sample kinetics of the emissions). In (A), the data for the first and the second emission burst of LOX and the sum of the two are separately shown and fitted by linear regressions (for the main panel,  $y=0.0112x-0.0124$  for the first and  $y=0.0716x+0.0322$  for the second LOX burst; for the inset,  $y=0.00576x-0.0080$  for the first and  $y=0.0409x+0.023$  for the second LOX burst). For  $I_{T, methanol}$  in (B) and for  $I_{T, monoterpene}$  in (C), the data were fitted by second-order polynomial regressions [for the main panels,  $y=0.0093x^2+0.99x+1.62$  for (B) and  $y=0.22x^2+9.43x+15.2$  for (C); and for the insets,  $y=0.0026x^2+0.25x+2.66$  for (B) and  $y=0.12x^2+3.85x+17.8$  for (C)]. For  $I_{T, sesquiterpene}$  in (D), the data were fitted by sigmoidal regressions [ $y=127/[1+e^{(11.3-x)/4.20}]$  for the main panel and  $y=161/[1+e^{(25.8-x)/9.16}]$  for the inset]. MeJA treatment is as in Fig. 1. For all relationships in (A) and (B) and for the main panel of (C),  $r^2=0.99$ ,  $P<0.001$ . For the inset of (C),  $r^2=0.98$ ,  $P<0.01$  and for the main panel and the inset of (D),  $r^2=0.96$ ,  $P<0.01$ . Three replicate treatments at each MeJA application concentration were carried out.

inducible terpenoid synthases not expressed under non-stressed conditions. The terpenoids elicited by MeJA in our study (Table 2), especially monoterpenes (limonene and linalool) and sesquiterpenes ( $\beta$ -farnesene,  $\alpha$ -cedrene, and  $\beta$ -caryophyllene), are also induced in herbivore-infested cucumber (Bouwmeester et al., 1999; Kappers et al., 2010), and play key roles as airborne signals attracting herbivore enemies or in priming defenses in neighboring plants (Degenhardt and Lincoln, 2006; Brill et al., 2009; Mäntylä et al., 2014).

As previous studies have demonstrated, biosynthesis of terpenes is delayed after the initiation of biotic stress (Arimura et al., 2008, 2009), reflecting the lags in signal transduction as well as the fact that the transcription and translation of terpene synthases are time-consuming. However, the existence of a second sustained burst of LOX compounds synchronously with the elicitation of induced terpene emissions after ~10 h is surprising. Because it occurred simultaneously with terpenoid emissions, this second burst of LOX compounds is unlikely to be the chemical elicitor inducing terpenoid release. In fact, there is evidence that the late MeJA response reflects the rise of endogenously synthesized jasmonate levels (Tamogami et al., 2008), and, thus, the second release of LOX might indicate the onset of jasmonate-dependent gene expression as reported in several previous studies for lipoxigenase

pathway genes (Bell and Mullet, 1991; Wasternack and Parthier, 2007).

From a biological perspective, LOX compounds are not only released upon immediate wounding in herbivore-damaged leaves, but also concomitantly with the synthesis of terpenoids elicited at the later stages of induction. Moreover, these LOX-containing compound blends play important roles in attraction of herbivore enemies and in priming of neighboring plants (Dicke et al., 1999; Bruinsma et al., 2007; Frost et al., 2008; Allmann and Baldwin, 2010; Copolovici et al., 2011, 2014a). Although the exposure to MeJA does not fully mimic the herbivory stress (Dicke et al., 1999; Degenhardt and Lincoln, 2006; Kappers et al., 2010), it still elicits a blend of volatiles that attracts enemies of herbivores similarly to genuine herbivore feeding (Dicke et al., 1999; Kappers et al., 2010). Thus, this second LOX burst concomitant with the induced terpenoid emissions might be part of the characteristic herbivory smell bouquet that is driving the plant–insect and plant–plant interactions.

Although longer term kinetic studies are rare, especially those considering the entire bouquet of volatiles, biphasic emission kinetics have been demonstrated in response to various stresses for several volatiles, including biphasic methanol emissions upon ozone stress (Beauchamp et al., 2005), biphasic ethylene emissions in response to treatments with the

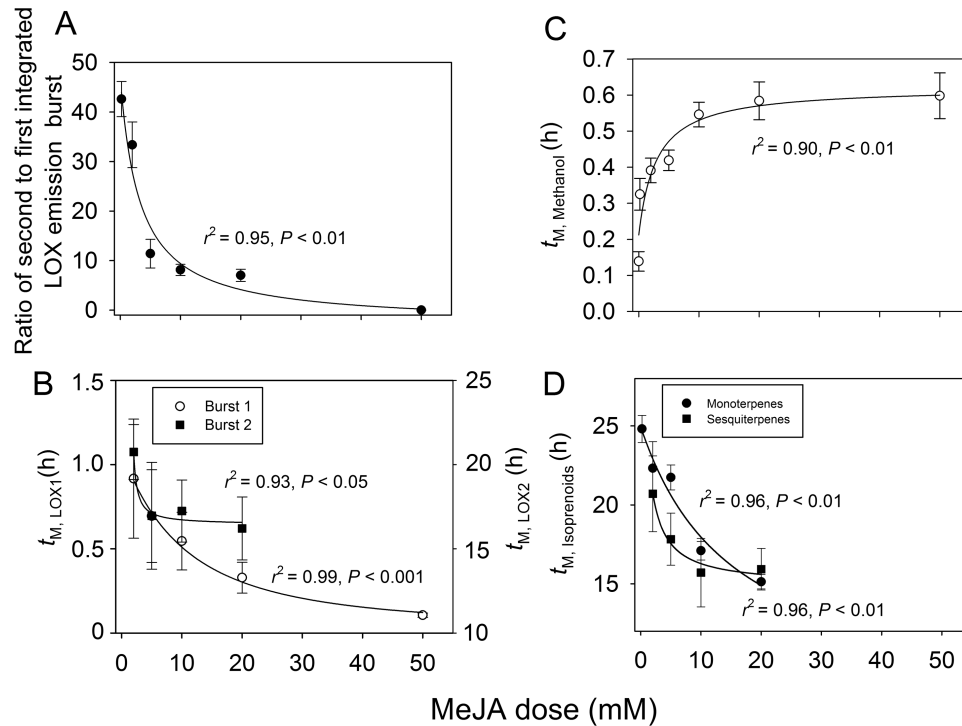


**Fig. 5.** The ratio of the second to the first integrated LOX emission burst ( $t_{\text{LOX2}}/t_{\text{LOX1}}$ , A), and the times to the maxima of the first ( $t_{\text{M,LOX1}}$ ) and second ( $t_{\text{M,LOX2}}$ ) LOX emission bursts (B), emission burst of methanol (C) and the times to the maxima of monoterpene ( $t_{\text{M,monoterpene}}$ ) and sesquiterpene ( $t_{\text{M,sesquiterpene}}$ ) emission bursts (D) in relation to MeJA dose in leaves of *C. sativus* (see Fig. 2 for the sample responses and definition of the characteristics). MeJA treatments are as in Fig. 1 and data coverage is as in Fig. 3. In all cases, the data were fitted by hyperbolic regressions. For  $t_{\text{LOX2}}/t_{\text{LOX1}}$  in (A),  $y=162/(3.27+x)-2.83$ ,  $r^2=0.95$ ,  $P<0.01$ ; for  $t_{\text{M,LOX1}}$  in (B),  $y=14.1/(11.7+x)-0.12$ ,  $r^2=0.99$ ,  $P<0.001$ ; for  $t_{\text{M,LOX2}}$  in (B),  $y=9.69/(0.0027+x)+15.7$ ,  $r^2=0.93$ ,  $P<0.01$ ; for  $t_{\text{M,methanol}}$  in (C),  $y=0.41x/(2.90+x)+0.21$ ; for  $t_{\text{M,monoterpene}}$  in (D),  $y=281/(15.7+x)+7.03$ ,  $r^2=0.96$ ,  $P<0.01$ ; for  $t_{\text{M,sesquiterpene}}$  in (D),  $y=14.6/(0.50+x)+14.9$ ,  $r^2=0.96$ ,  $P<0.01$ . Three replicate treatments at each MeJA application concentration were carried out.

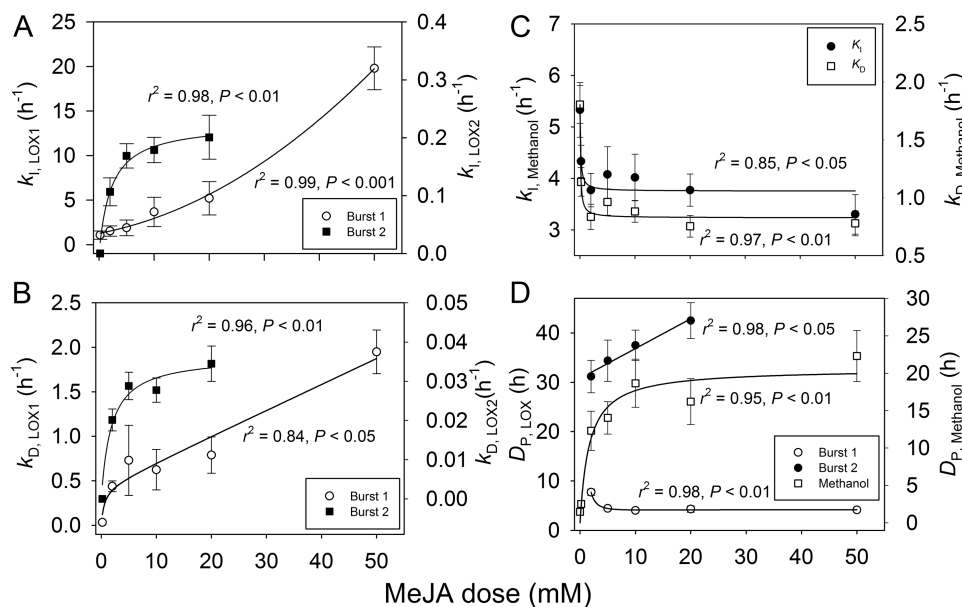


**Fig. 6.** First-order rate constants ( $k_i$ ) for the initial increases (Equation 2,  $k_i$ ; A, C) and decreases (Equation 3,  $k_D$ ; B, C) of the MeJA-induced emissions for the first ( $k_{i,\text{LOX1}}$  and  $k_{D,\text{LOX1}}$ ) and the second ( $k_{i,\text{LOX2}}$  and  $k_{D,\text{LOX2}}$ ) emission burst of LOX volatiles (A, B) and methanol (C), and the duration ( $D_P$ ) of the first and second LOX compound emission burst and methanol emission burst (D) as dependent on the MeJA concentration in *C. sativus* leaves (see Fig. 2 for sample responses). Experimental treatments are as in Fig. 1 and data coverage is as in Fig. 3. The regressions describing the statistical effects of MeJA on the rate constants were the following:  $y=0.0050x^2+0.12x+1.27$  for  $k_{i,\text{LOX1}}$  and  $y=0.214x/(1.87+x)$  for  $k_{i,\text{LOX2}}$  in (A),  $y=2.51(1-e^{-0.028x})$  for  $k_{D,\text{LOX1}}$  and  $y=0.0357x/(1.42+x)$  for  $k_{D,\text{LOX2}}$  in (B),  $y=3.75+0.194/(0.123+x)$  for  $k_{i,\text{methanol}}$  and  $y=0.826+0.0920/(0.094+x)$  for  $k_{D,\text{methanol}}$  in (C),  $y=4.24-3.11/x+20.1/x^2$  for  $D_{P,\text{LOX1}}$ ,  $y=30.8+0.604x$  for  $D_{P,\text{LOX2}}$ , and  $y=20.6x/(1.65+x)$  for  $D_{P,\text{methanol}}$  in (D). Three replicate treatments at each MeJA application concentration were carried out.

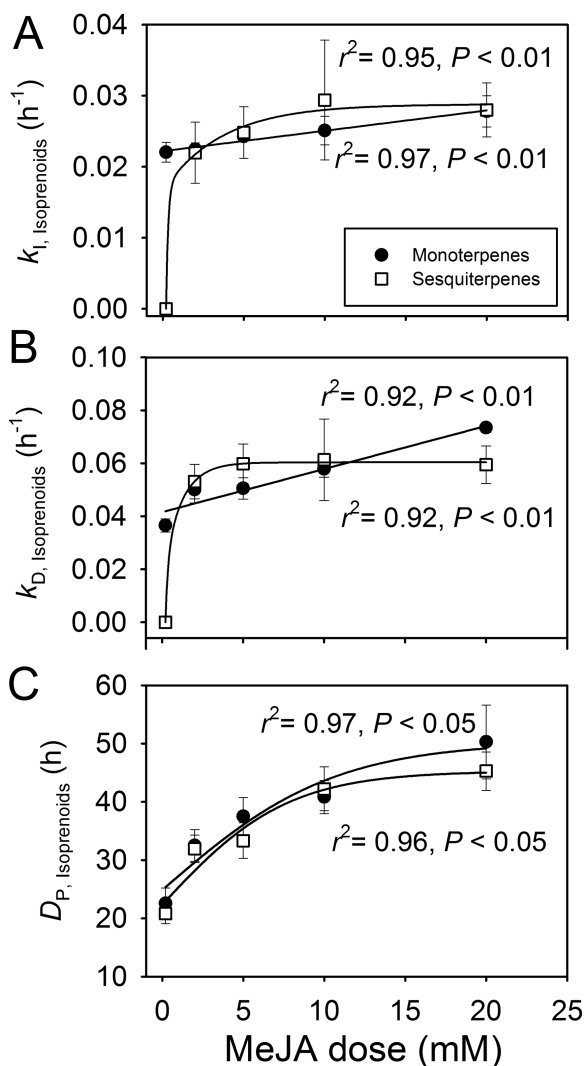


**Fig. 7.** First-order rate constants ( $k_i$ ) for the initial increases (Equation 2,  $k_i$ ; A) and decreases (Equation 3,  $k_D$ ; B) of the MeJA-induced emissions for mono- ( $k_{i, \text{monoterpene}}$  and  $k_{D, \text{monoterpene}}$ ) and sesquiterpenes ( $k_{i, \text{sesquiterpene}}$  and  $k_{D, \text{sesquiterpene}}$ ) and the durations (C) of monoterpene ( $D_{P, \text{monoterpene}}$ ) and sesquiterpene ( $D_{P, \text{sesquiterpene}}$ ) emission bursts in relation to MeJA concentration in *C. sativus* leaves (see Fig. 2 for sample responses). Experimental treatments are as in Fig. 1 and data availability is as in Fig. 3. The regressions fitted to the data as:  $y=0.0029x+0.22$  for  $k_{i, \text{monoterpene}}$  and  $y=0.297x/(0.736+x)$  for  $k_{i, \text{sesquiterpene}}$  in (A),  $y=0.0016x+0.041$  for  $k_{D, \text{monoterpene}}$  and  $y=0.061x/(0.295+x)$  for  $k_{D, \text{sesquiterpene}}$  in (B),  $y=50.3/[1+e^{(0.107-x)/5.26}]$  for  $D_{P, \text{monoterpene}}$  and  $y=45.3/[1+e^{(0.0784-x)/3.84}]$  for  $D_{P, \text{sesquiterpene}}$  in (C). Altogether three replicate treatments at each MeJA application concentration were carried out.

fungal elicitor cryptogin and infections by *Phytophthora parasitica* (Wi et al., 2012) and *Pseudomonas syringae* (Mur et al., 2008), and biphasic LOX product and terpenoid emissions in response to infections by *Melampsora epitea* (Toome et al., 2010). However, with the exception of the ozone stress study of Beauchamp et al. (2005) that was carried out with a proton-transfer reaction quadrupole mass spectrometer (PTR-QMS), other kinetic studies had much lower time resolution than that (10 s) used in our study. While the elicitation of the volatile response to mechanical wounding and herbivory is characteristically very fast (Brilli et al., 2011; Copolovici et

al., 2011, 2014a; Portillo-Estrada et al., 2015), resembling the MeJA treatment response in our study, both the first and the second emission bursts in the pathogen-infected leaves (Mur et al., 2008; Toome et al., 2010; Wi et al., 2012) occurred later than in our study in MeJA-treated leaves (Fig. 2A, D). Clearly, different stresses can propagate differently, reflecting the diversity of biological characteristics of impacting organisms as well as differences in stress perception and signal transduction. Further research using high-resolution techniques as used here is needed to resolve the general and specific features of shorter and longer term elicitation responses induced by different stresses, including studies linking the emissions to pertinent gene expression patterns.

#### Emission rates and total emission of induced volatiles scale with MeJA dose

The level of biological stress varies greatly depending on the degree of infestation by herbivores and infection by pathogens (Niinemets et al., 2013), but biological stress severity versus stress response relationships have not been routinely studied. Here we observed that MeJA treatment concentration and the degree of leaf area damaged were quantitatively correlated (Fig. 1), in agreement with past observations indicating that exogenous application of MeJA can result in local phytotoxicity (Hejari et al., 2005). We also observed that both the total and maximum emissions of LOX compounds for both the early and the second emission burst (Figs 3A, 4A), for the early methanol emission burst (Figs 3B, 4B), and for the late monoterpene (Figs 3C, 4C) and sesquiterpene (Figs 3D, 4D) emission bursts were quantitatively associated with MeJA concentration and the proportion of leaf area damaged (damage severity). Thus, these results indicate that both the initial stress response due to activation of constitutive defenses and the later response due to activation of induced defenses are dose dependent.

MeJA that mainly enters through the stomata, and to a lower degree through the cuticle, is expected to become progressively diluted as it penetrates deeper into the leaf interior and dissolves in leaf water. Thus, the dose dependence of the early constitutive response as evident in the first LOX compound burst (Fig. 2A) and in the methanol burst (Fig. 2D) can result from quantitative scaling of the proportion of impacted cell wall and membrane sites with MeJA concentration. Such a positive scaling of early LOX and methanol emission responses with the degree of impact has been observed in wounding experiments (Brilli et al., 2011; Portillo-Estrada et al., 2015), and suggests that the control of the rapid elicitation response at the level of immediate impact is possible.

In the case of the late-induced response, the situation is less clear because in addition to MeJA *per se*, the primary MeJA-induced LOX volatile emissions can propagate the signal to cellular locations not necessarily directly impacted by MeJA (Cardoza et al., 2002; Engelberth et al., 2007; Kishimoto et al., 2008; Piesik et al., 2013; Castelyn et al., 2015).

The MeJA dose dependence of induced emissions resembles herbivory experiments where the rate of emissions of mono- and sesquiterpenes increases with the proportion of



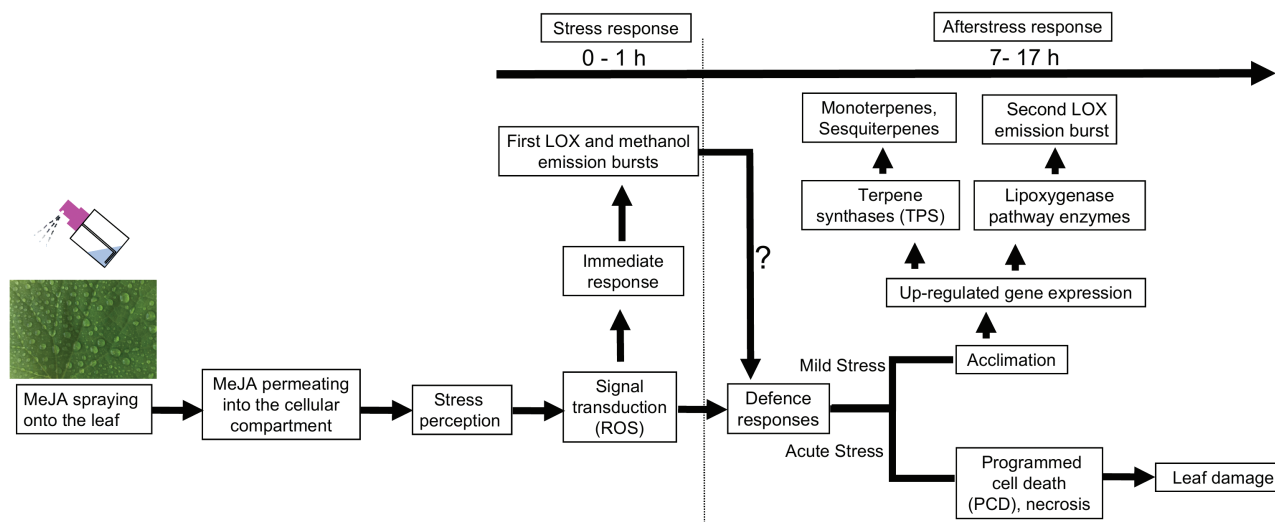


**Fig. 8.** A conceptual model of elicitation of short- and long-term volatile responses upon MeJA treatment of cucumber leaves. Gaseous MeJA is taken up into the leaf internal air space through stomata, permeates further through cell walls and plasmalemma, reaching ultimately the symplastic leaf compartments. This activates an oxidative burst due to rapid formation of reactive oxygen species (ROS; Garrido *et al.*, 2003; Zhang and Xing, 2008; Küpper *et al.*, 2009; Hazra *et al.*, 2017) and release of free polyunsaturated fatty acids from plant membranes (Dicke *et al.*, 1999; Feussner and Wasternack, 2002; Andreou and Feussner, 2009) in several minutes after the treatment at the immediate location of MeJA impact. Due to the constitutive activity of lipoxygenases, free fatty acids are rapidly converted to volatile lipoxygenase pathway products (LOX products; Feussner and Wasternack, 2002; Andreou and Feussner, 2009), resulting in the first burst of LOX emissions (Fig. 2A). Simultaneously with the release of free fatty acids or maybe even somewhat earlier, constitutive pectin methylesterases (Michell, 2001; Pelloux *et al.*, 2007) are activated, resulting in major emissions of methanol (Fig. 2D). In a longer-term sequence of events probably involving endogenous jasmonate formation and interplay with jasmonate repressor proteins (JAZ) (Chini *et al.*, 2007; Wasternack and Song, 2017; Zhang *et al.*, 2017), plant defense responses depend on the initial stress severity. Mild and moderate stress caused by MeJA treatment (5, 10, and 20 mM) is expected to lead to elicitation of gene expression level defenses including enhanced expression of terpenoid synthase (TPS; Martin *et al.*, 2002, 2003; Byun-McKay *et al.*, 2006) and lipoxygenase pathway genes (Bell and Mullet, 1991; Wasternack and Parthier, 2007), resulting in volatile terpene and LOX emissions that are sustained for long time periods of ~20–30 h (Fig. 2B, C). In the case of moderate stress, propagation of necrotic lesions remains localized (Fig. 1A). In contrast, acute MeJA stress (50 mM) leads to enhanced progression of programmed cell death (PCD), and subsequent rapid propagation of necrosis over the entire leaf surface (Fig. 1A).

leaf area consumed (Copolovici *et al.*, 2011, 2014a), indicating that the rate of terpene synthesis becomes progressively greater in the remaining tissues. Analogously, in fungal-infected leaves, terpenoid emissions increase with increasing spread of the necrotic area (Jiang *et al.*, 2016b). We argue that the quantitative relationships between the dose of the model compound MeJA, severity of damage, and the volatile emission responses in cucumber have major biological consequences. Studies have demonstrated that different levels of induction of volatiles by MeJA treatment alter both plant attractiveness to herbivores (Heil, 2014) and the repellency to herbivores (Zas *et al.*, 2011). This suggests that the capacity to respond to a biotic stress in a dose-dependent manner as demonstrated here provides significant fitness advantages.

#### *A conceptual model describing MeJA elicitation of defenses from stress response to acclimation*

The induction of volatiles released upon MeJA treatment from cucumber leaves followed similar elicitation patterns for both the fast and slow phases, with an initial exponential or sigmoidal increase to a maximum level, followed by a decrease to the baseline emission (Fig. 2). We fitted the temporal shapes of the increase and decrease of volatiles by first-order exponential relationships to characterize the rise and decay kinetics (Equations 2 and 3) and further characterized

the timing of emission elicitation (Fig. 2; Table 1). Both the rate of increase and the decrease of LOX compounds and terpenoids were strongly enhanced by increasing MeJA concentrations (Figs 6A, B, 7A, B). Furthermore, both the first and the second LOX burst (Fig. 5B) and monoterpene and sesquiterpene emission bursts (Fig. 5D) occurred earlier, and were sustained for longer time periods (Figs 6D, 7C) at higher MeJA dose. This evidence emphasizes the highly dynamic nature of the MeJA concentration dependence of volatile emissions over both the short and long term.

For chronic biotic stresses such as herbivory infestation and pathogen attacks, quantitative relationships between the severity of biotic stress and release of induced volatiles have been suggested to result from the scaling of emissions with propagation of damage and the number of simultaneous stress impact sites (Niinemets *et al.*, 2013). As this study with MeJA elicitor demonstrates, the scaling relationships of volatile responses with MeJA dose, the ‘stress severity’, consist of both local and systemic responses. As for the local early response, it indeed can reflect scaling of emissions with the spread of the immediate stress impact sites (Fig. 8). However, the quantitative scaling of the subsequent slower gene-level responses with MeJA dose is obviously more complex and probably reflects a systemic response. The timing and magnitude of this systemic response is determined by the initial MeJA dose, but the way in which the early stress signal

determines the gene expression response is still unclear at a mechanistic level, and will require further studies looking at both the activation of expression of regulator and target genes. It is likely that the balance between the free transcription regulator MYC2 that activates downstream jasmonate transcriptional responses and jasmonate signaling repressor proteins (JAZ proteins) that negatively affect MYC2 levels (Gális *et al.*, 2009), together with the elicitation of endogenous jasmonate synthesis (Tamogami *et al.*, 2008), determines the onset of elicitation of gene expression and subsequent repression.

Furthermore, the set of events downstream of the initial MeJA impact consists of acclimation responses and localized acute necrotic or PCD-like responses with the share among them determined by the initial MeJA concentration (Figs 1, 8). Thus, with increasing MeJA concentration, a greater proportion of leaf area undergoes death, while the volatile emission capacity of the remaining cells is increasingly up-regulated. Stronger amplification of the emission capacity in those cells still alive resembles the emission response to herbivory where foliar terpenoid emissions in remaining leaf parts increase dependent on the proportion of leaf area consumed by herbivores (Copolovici *et al.*, 2011, 2014a, 2017).

What could be the biological significance of the dose dependence of the second elicited emission burst? Due to high reactivity in the ambient atmosphere, the volatile signal itself fades with the distance from the emission source (Holopainen and Blande, 2013; Holopainen *et al.*, 2013; Blande *et al.*, 2014). Thus, a stronger signal will reach more distant leaves, and also provides a farther reaching signal for other organisms such as herbivore predators. Furthermore, we suggest that the strength of the volatile signal might carry information about the severity of the biological impact and, as such, contribute to stronger priming responses in surrounding leaves of the same plant and neighboring plants. We argue that for quantitative prediction of biotic stress severity versus emission response relationships, further studies are needed to gain insight into the turnover of JAZ and MYC2 proteins and into the timing and magnitude of formation of endogenous jasmonate as driven by the severity of biotic stress impact.

## Conclusions

High time resolution measurements conducted here have highlighted the biphasic kinetics of volatile emissions induced by MeJA treatment. Our study demonstrates rapid constitutive lipoxygenase pathway volatile (LOX) and methanol emissions and subsequent elicitation of terpenoid emission. Strong quantitative relationships between the timing and magnitude of early and late emissions and applied MeJA concentration collectively indicate high plant plastic capacity to respond to biotic stress, and emphasize the highly dynamic nature of the MeJA concentration dependence of volatile emissions over both the short and long term. Albeit that this study presented exciting evidence of quantitative scaling of local and systemic emission responses to MeJA treatment, we suggest that to gain insight into the mechanisms of regulation of the magnitude and kinetics of the downstream responses

and validate the differences in the sensitivity of gene expression in cucumber, further studies should look at expression of terpenoid synthase genes under treatments with different MeJA concentrations. In addition, higher resolution reactive oxygen species measurement techniques should be developed to obtain complementary information on leaf oxidative status through the emissions bursts recorded by PTR-TOF-MS.

## Acknowledgements

We acknowledge the financial support from the European Commission through the European Research Council (advanced grant 322603, SIP-VOL+), the European Regional Development Fund (Centre of Excellence EcolChange), and the Estonian Ministry of Science and Education (institutional grant IUT-8-3).

## References

- Adams RP. 1995. Identification of essential oil components by gas chromatography and mass spectrometry, 3rd edn. USA: Allured Publishing Corporation.
- Allmann S, Baldwin IT. 2010. Insects betray themselves in nature to predators by rapid isomerization of green leaf volatiles. *Science* **329**, 1075–1078.
- Andreou A, Feussner I. 2009. Lipoxygenases—structure and reaction mechanism. *Phytochemistry* **70**, 1504–1510.
- Arimura G, Matsui K, Takabayashi J. 2009. Chemical and molecular ecology of herbivore-induced plant volatiles: proximate factors and their ultimate functions. *Plant and Cell Physiology* **50**, 911–923.
- Arimura G, Garms S, Maffei M, Bossi S, Schulze B, Leitner M, Mithöfer A, Boland W. 2008. Herbivore-induced terpenoid emission in *Medicago truncatula*: concerted action of jasmonate, ethylene and calcium signaling. *Planta* **227**, 453–464.
- Beauchamp J, Wisthaler A, Hansel A, Kleist E, Miebach M, Niinemets Ü, Schurr U, Wildt J. 2005. Ozone induced emissions of biogenic VOC from tobacco: relations between ozone uptake and emission of LOX products. *Plant, Cell and Environment* **28**, 1334–1343.
- Bell E, Mullet JE. 1991. Lipoxygenase gene expression is modulated in plants by water deficit, wounding, and methyl jasmonate. *Molecular and General Genetics* **230**, 456–462.
- Blande JD, Holopainen JK, Niinemets Ü. 2014. Plant volatiles in polluted atmospheres: stress responses and signal degradation. *Plant, Cell and Environment* **37**, 1892–1904.
- Bouwmeester HJ, Verstappen FW, Posthumus MA, Dicke M. 1999. Spider mite-induced (3S)-(*E*)-nerolidol synthase activity in cucumber and lima bean. The first dedicated step in acyclic C11-homoterpene biosynthesis. *Plant Physiology* **121**, 173–180.
- Brilli F, Ciccio P, Frattoni M, Prestininzi M, Spanedda AF, Loreto F. 2009. Constitutive and herbivore-induced monoterpenes emitted by *Populus × euroamericana* leaves are key volatiles that orient *Chrysomela populi* beetles. *Plant, Cell and Environment* **32**, 542–552.
- Brilli F, Ruuskanen TM, Schnitzhofer R, Müller M, Breitenlechner M, Bittner V, Wohlfahrt G, Loreto F, Hansel A. 2011. Detection of plant volatiles after leaf wounding and darkening by proton transfer reaction 'time-of-flight' mass spectrometry (PTR-TOF). *PLoS One* **6**, e20419.
- Bruinsma M, Posthumus MA, Mumm R, Mueller MJ, van Loon JJ, Dicke M. 2009. Jasmonic acid-induced volatiles of *Brassica oleracea* attract parasitoids: effects of time and dose, and comparison with induction by herbivores. *Journal of Experimental Botany* **60**, 2575–2587.
- Bruinsma M, Van Dam NM, Van Loon JJ, Dicke M. 2007. Jasmonic acid-induced changes in *Brassica oleracea* affect oviposition preference of two specialist herbivores. *Journal of Chemical Ecology* **33**, 655–668.
- Byun-McKay A, Godard KA, Toudefallah M, Martin DM, Alfaro R, King J, Bohlmann J, Plant AL. 2006. Wound-induced terpene synthase gene expression in Sitka spruce that exhibit resistance or susceptibility to attack by the white pine weevil. *Plant Physiology* **140**, 1009–1021.
- Cardoza YJ, Alborn HT, Tumlinson JH. 2002. In vivo volatile emissions from peanut plants induced by simultaneous fungal infection and insect damage. *Journal of Chemical Ecology* **28**, 161–174.

- Castelyn HD, Appelgryn JJ, Mafa MS, Pretorius ZA, Visser B. 2015. Volatiles emitted by leaf rust infected wheat induce a defence response in exposed uninfected wheat seedlings. *Australas Plant Pathology* **44**, 245–254.
- Cheong JJ, Choi YD. 2003. Methyl jasmonate as a vital substance in plants. *Trends in Genetics: TIG* **19**, 409–413.
- Chini A, Fonseca S, Fernández G, *et al.* 2007. The JAZ family of repressors is the missing link in jasmonate signalling. *Nature* **448**, 666–671.
- Copolovici LO, Filella I, Llusà J, Niinemets Ü, Peñuelas J. 2005. The capacity for thermal protection of photosynthetic electron transport varies for different monoterpenes in *Quercus ilex*. *Plant Physiology* **139**, 485–496.
- Copolovici L, Kännaste A, Pazouki L, Niinemets Ü. 2012. Emissions of green leaf volatiles and terpenoids from *Solanum lycopersicum* are quantitatively related to the severity of cold and heat shock treatments. *Journal of Plant Physiology* **169**, 664–672.
- Copolovici L, Kännaste A, Rimmel T, Niinemets Ü. 2014a. Volatile organic compound emissions from *Alnus glutinosa* under interacting drought and herbivory stresses. *Environmental and Experimental Botany* **100**, 55–63.
- Copolovici L, Kännaste A, Rimmel T, Vislap V, Niinemets Ü. 2011. Volatile emissions from *Alnus glutinosa* induced by herbivory are quantitatively related to the extent of damage. *Journal of Chemical Ecology* **37**, 18–28.
- Copolovici L, Niinemets Ü. 2010. Flooding induced emissions of volatile signalling compounds in three tree species with differing waterlogging tolerance. *Plant, Cell and Environment* **33**, 1582–1594.
- Copolovici L, Pag A, Kännaste A, Bodescu A, Tomescu D, Copolovici D, Soran ML, Niinemets Ü. 2017. Disproportionate photosynthetic decline and inverse relationship between constitutive and induced volatile emissions upon feeding of *Quercus robur* leaves by large larvae of gypsy moth (*Lymantria dispar*). *Environmental and Experimental Botany* **138**, 184–192.
- Copolovici L, Väärtnõu F, Portillo Estrada M, Niinemets Ü. 2014b. Oak powdery mildew (*Erysiphe alphitoides*)-induced volatile emissions scale with the degree of infection in *Quercus robur*. *Tree Physiology* **34**, 1399–1410.
- Degenhardt DC, Lincoln DE. 2006. Volatile emissions from an odorous plant in response to herbivory and methyl jasmonate exposure. *Journal of Chemical Ecology* **32**, 725–743.
- Dicke M, Gols R, Ludeking D, Posthumus MA. 1999. Jasmonic acid and herbivory differentially induce carnivore-attracting plant volatiles in lima bean plants. *Journal of Chemical Ecology* **25**, 1907–1922.
- Engelberth J, Seidl-Adams I, Schultz JC, Tumlinson JH. 2007. Insect elicitors and exposure to green leafy volatiles differentially upregulate major octadecanoids and transcripts of 12-oxo phytodienoic acid reductases in *Zea mays*. *Molecular Plant-Microbe Interactions* **20**, 707–716.
- Farag MA, Paré PW. 2002. C6-Green leaf volatiles trigger local and systemic VOC emissions in tomato. *Phytochemistry* **61**, 545–554.
- Feussner I, Wasternack C. 2002. The lipoxygenase pathway. *Annual Review of Plant Biology* **53**, 275–297.
- Frost CJ, Mescher MC, Dervinis C, Davis JM, Carlson JE, De Moraes CM. 2008. Priming defense genes and metabolites in hybrid poplar by the green leaf volatile *cis*-3-hexenyl acetate. *New Phytologist* **180**, 722–734.
- Gális I, Gaquerel E, Pandey SP, Baldwin IT. 2009. Molecular mechanisms underlying plant memory in JA-mediated defence responses. *Plant, Cell and Environment* **32**, 617–627.
- Gao H, Zhu H, Shao Y, Chen A, Lu C, Zhu B, Luo Y. 2008. Lycopene accumulation affects the biosynthesis of some carotenoid-related volatiles independent of ethylene in tomato. *Journal of Integrative Plant Biology* **50**, 991–996.
- Garrido I, Espinosa F, Córdoba-Pedregosa MC, González-Reyes JA, Alvarez-Tinaut MC. 2003. Redox-related peroxidative responses evoked by methyl-jasmonate in axenically cultured aeroponic sunflower (*Helianthus annuus* L.) seedling roots. *Protoplasma* **221**, 79–91.
- Grote R, Monson RK, Niinemets Ü. 2013. Leaf-level models of constitutive and stress-driven volatile organic compound emissions. In: Niinemets Ü, Monson RK, eds. *Biology, controls and models of tree volatile organic compound emissions*. Tree Physiology 5. Berlin: Springer, 315–355.
- Hann CT, Bequette CJ, Dombrowski JE, Stratmann JW. 2014. Methanol and ethanol modulate responses to danger- and microbe-associated molecular patterns. *Frontiers in Plant Science* **5**, 550.
- Hazra S, Bhattacharyya D, Chattopadhyay S. 2017. Methyl jasmonate regulates podophyllotoxin accumulation in *Podophyllum hexandrum* by altering the ROS-responsive podophyllotoxin pathway gene expression additionally through the down regulation of few interfering miRNAs. *Frontiers in Plant Science* **8**, 164.
- Heijari J, Nerg AM, Kainulainen P, Viiri H, Vuorinen M, Holopainen JK. 2005. Application of methyl jasmonate reduces growth but increases chemical defence and resistance against *Hylobius abietis* in Scots pine seedlings. *Entomologia Experimentalis et Applicata* **115**, 117–124.
- Heijari J, Nerg AM, Kainulainen P, Vuorinen M, Holopainen JK. 2008. Long-term effects of exogenous methyl jasmonate application on Scots pine (*Pinus sylvestris*) needle chemical defence and diprionid sawfly performance. *Entomologia Experimentalis et Applicata* **128**, 162–171.
- Heil M. 2014. Herbivore-induced plant volatiles: targets, perception and unanswered questions. *New Phytologist* **204**, 297–306.
- Heil M, Kost C. 2006. Priming of indirect defences. *Ecology Letters* **9**, 813–817.
- Heil M, Ton J. 2008. Long-distance signalling in plant defence. *Trends in Plant Science* **13**, 264–272.
- Holopainen JK, Blande JD. 2013. Where do herbivore-induced plant volatiles go? *Frontiers in Plant Science* **4**, 185.
- Holopainen JK, Nerg AM, Blande JD. 2013. Multitrophic signalling in polluted atmospheres. In: Niinemets Ü, Monson RK, eds. *Biology, controls and models of tree volatile organic compound emissions*. Tree Physiology 5. Berlin: Springer, 285–314.
- Hu ZH, Shen YB, Su XH. 2009. Saturated aldehydes C<sub>6</sub>–C<sub>10</sub> emitted from ashleaf maple (*Acer negundo* L.) leaves at different levels of light intensity, O<sub>2</sub>, and CO<sub>2</sub>. *Journal of Plant Biology* **52**, 289–298.
- Jiang Y, Ye J, Li S, Niinemets Ü. 2016a. Regulation of floral terpenoid emission and biosynthesis in sweet basil (*Ocimum basilicum*). *Journal of Plant Growth Regulation* **35**, 921–935.
- Jiang Y, Ye J, Veromann LL, Niinemets Ü. 2016b. Scaling of photosynthesis and constitutive and induced volatile emissions with severity of leaf infection by rust fungus (*Melampsora larici-populina*) in *Populus balsamifera* var. *suaveolens*. *Tree Physiology* **36**, 856–872.
- Jonak C, Okrész L, Bögre L, Hirt H. 2002. Complexity, cross talk and integration of plant MAP kinase signalling. *Current Opinion in Plant Biology* **5**, 415–424.
- Jung S. 2004. Effect of chlorophyll reduction in *Arabidopsis thaliana* by methyl jasmonate or norflurazon on antioxidant systems. *Plant Physiology and Biochemistry* **42**, 225–231.
- Kännaste A, Copolovici L, Niinemets Ü. 2014. Gas chromatography mass-spectrometry method for determination of biogenic volatile organic compounds emitted by plants. *Methods in Molecular Biology* **1153**, 161–169.
- Kappers IF, Verstappen FW, Luckerhoff LL, Bouwmeester HJ, Dicke M. 2010. Genetic variation in jasmonic acid- and spider mite-induced plant volatile emission of cucumber accessions and attraction of the predator *Phytoseiulus persimilis*. *Journal of Chemical Ecology* **36**, 500–512.
- Kask K, Kännaste A, Talts E, Copolovici L, Niinemets Ü. 2016. How specialized volatiles respond to chronic and short-term physiological and shock heat stress in *Brassica nigra*. *Plant, Cell and Environment* **39**, 2027–2042.
- Kegge W, Weldegergis BT, Soler R, Vergeer-Van Eijk M, Dicke M, Voesenek LA, Pierik R. 2013. Canopy light cues affect emission of constitutive and methyl jasmonate-induced volatile organic compounds in *Arabidopsis thaliana*. *New Phytologist* **200**, 861–874.
- Kishimoto K, Matsui K, Ozawa R, Takabayashi J. 2008. Direct fungicidal activities of C6-aldehydes are important constituents for defense responses in *Arabidopsis* against *Botrytis cinerea*. *Phytochemistry* **69**, 2127–2132.
- Komarova TV, Sheshukova EV, Dorokhov YL. 2014. Cell wall methanol as a signal in plant immunity. *Frontiers in Plant Science* **5**, 101.
- Küpper FC, Gaquerel E, Cosse A, Adas F, Peters AF, Müller DG, Kloareg B, Salaün JP, Potin P. 2009. Free fatty acids and methyl jasmonate trigger defense reactions in *Laminaria digitata*. *Plant and Cell Physiology* **50**, 789–800.
- Liang YS, Kim HK, Lefebvre AW, Erkelens C, Choi YH, Verpoorte R. 2006. Identification of phenylpropanoids in methyl jasmonate treated *Brassica rapa* leaves using two-dimensional nuclear magnetic resonance spectroscopy. *Journal of Chromatography A* **1112**, 148–155.



- Loivamäki M, Holopainen JK, Nerg AM.** 2004. Chemical changes induced by methyl jasmonate in oilseed rape grown in the laboratory and in the field. *Journal of Agricultural and Food Chemistry* **52**, 7607–7613.
- Mäntylä E, Blande JD, Klemola T.** 2014. Does application of methyl jasmonate to birch mimic herbivory and attract insectivorous birds in nature? *Arthropod-Plant Interactions* **8**, 143–153.
- Martin DM, Gershenzon J, Bohlmann J.** 2003. Induction of volatile terpene biosynthesis and diurnal emission by methyl jasmonate in foliage of Norway spruce. *Plant Physiology* **132**, 1586–1599.
- Martin D, Tholl D, Gershenzon J, Bohlmann J.** 2002. Methyl jasmonate induces traumatic resin ducts, terpenoid resin biosynthesis, and terpenoid accumulation in developing xylem of Norway spruce stems. *Plant Physiology* **129**, 1003–1018.
- Matsui K, Sugimoto K, Mano J, Ozawa R, Takabayashi J.** 2012. Differential metabolisms of green leaf volatiles in injured and intact parts of a wounded leaf meet distinct ecophysiological requirements. *PLoS One* **7**, e36433.
- Micheli F.** 2001. Pectin methylesterases: cell wall enzymes with important roles in plant physiology. *Trends in Plant Science* **6**, 414–419.
- Mithöfer A, Wanner G, Boland W.** 2005. Effects of feeding *Spodoptera littoralis* on lima bean leaves. II. Continuous mechanical wounding resembling insect feeding is sufficient to elicit herbivory-related volatile emission. *Plant Physiology* **137**, 1160–1168.
- Mur LA, Laarhoven LJ, Harren FJ, Hall MA, Smith AR.** 2008. Nitric oxide interacts with salicylate to regulate biphasic ethylene production during the hypersensitive response. *Plant Physiology* **148**, 1537–1546.
- Niinemets Ü.** 2010. Mild versus severe stress and BVOCs: thresholds, priming and consequences. *Trends in Plant Science* **15**, 145–153.
- Niinemets Ü, Kännaste A, Copolovici L.** 2013. Quantitative patterns between plant volatile emissions induced by biotic stresses and the degree of damage. *Frontiers in Plant Science* **4**, 262.
- Niinemets Ü, Kuhn U, Harley PC, et al.** 2011. Estimations of isoprenoid emission capacity from enclosure studies: measurements, data processing, quality and standardized measurement protocols. *Biogeosciences* **8**, 2209–2246.
- Pazouki L, Memari HR, Kännaste A, Bichele R, Niinemets Ü.** 2015. Germacrene A synthase in yarrow (*Achillea millefolium*) is an enzyme with mixed substrate specificity: gene cloning, functional characterization and expression analysis. *Frontiers in Plant Science* **6**, 111.
- Pelloux J, Rustérucchi C, Mellerowicz EJ.** 2007. New insights into pectin methylesterase structure and function. *Trends in Plant Science* **12**, 267–277.
- Peñuelas J, Filella I, Stefanescu C, Llusià J.** 2005. Caterpillars of *Euphydryas aurinia* (Lepidoptera: Nymphalidae) feeding on *Succisa pratensis* leaves induce large foliar emissions of methanol. *New Phytologist* **167**, 851–857.
- Phillips MA, Walter MH, Ralph SG, et al.** 2007. Functional identification and differential expression of 1-deoxy-D-xylulose 5-phosphate synthase in induced terpenoid resin formation of Norway spruce (*Picea abies*). *Plant Molecular Biology* **65**, 243–257.
- Piesik D, Panka D, Jeske M, Wenda-Piesik A, Delaney KJ, Weaver DK.** 2013. Volatile induction of infected and neighbouring uninfected plants potentially influence attraction/repellence of a cereal herbivore. *Journal of Applied Entomology* **137**, 296–309.
- Popova LP, Ananieva E, Hristova V, Christov K, Georgieva K, Alexieva V, Stoinova ZH.** 2003. Salicylic acid- and methyl jasmonate-induced protection on photosynthesis to paraquat oxidative stress. *Bulgarian Journal of Plant Physiology Special issue*, 133–152.
- Portillo-Estrada M, Kazantsev T, Niinemets Ü.** 2017. Fading of wound-induced volatile release during *Populus tremula* leaf expansion. *Journal of Plant Research* **130**, 157–165.
- Portillo-Estrada M, Kazantsev T, Talts E, Tosens T, Niinemets Ü.** 2015. Emission timetable and quantitative patterns of wound-induced volatiles across different leaf damage treatments in aspen (*Populus tremula*). *Journal of Chemical Ecology* **41**, 1105–1117.
- Repka V, Cerna M, Pavlovkin J.** 2013. Methyl jasmonate-induced cell death in grapevine requires both lipoxygenase activity and functional octadecanoid biosynthetic pathway. *Biologia* **68**, 896–903.
- Rodriguez-Saona C, Crafts-Brandner SJ, Paré PW, Henneberry TJ.** 2001. Exogenous methyl jasmonate induces volatile emissions in cotton plants. *Journal of Chemical Ecology* **27**, 679–695.
- Scala A, Allmann S, Mirabella R, Haring MA, Schuurink RC.** 2013. Green leaf volatiles: a plant's multifunctional weapon against herbivores and pathogens. *International Journal of Molecular Sciences* **14**, 17781–17811.
- Seco R, Filella I, Llusià J, Peñuelas J.** 2011. Methanol as a signal triggering isoprenoid emissions and photosynthetic performance in *Quercus ilex*. *Acta Physiologiae Plantarum* **33**, 2413–2422.
- Semiz G, Blande JD, Heijari J, Işık K, Niinemets Ü, Holopainen JK.** 2012. Manipulation of VOC emissions with methyl jasmonate and carrageenan in the evergreen conifer *Pinus sylvestris* and evergreen broadleaf *Quercus ilex*. *Plant Biology* **14 Suppl 1**, 57–65.
- Shi J, Ma C, Qi D, Lv H, Yang T, Peng Q, Chen Z, Lin Z.** 2015. Transcriptional responses and flavor volatiles biosynthesis in methyl jasmonate-treated tea leaves. *BMC Plant Biology* **15**, 233.
- Suh HW, Hyun SH, Kim SH, Lee SY, Choi HK.** 2013. Metabolic profiling and enhanced production of phytochemicals by elicitation with methyl jasmonate and silver nitrate in whole plant cultures of *Lemna paucicostata*. *Process Biochemistry* **48**, 1581–1586.
- Tani A, Hayward S, Hewitt CN.** 2003. Measurement of monoterpenes and related compounds by proton transfer reaction-mass spectrometry (PTR-MS). *International Journal of Mass Spectrometry* **223–224**, 561–578.
- Tamogami S, Rakwal R, Agrawal GK.** 2008. Interplant communication: airborne methyl jasmonate is essentially converted into JA and JA-Ile activating jasmonate signaling pathway and VOCs emission. *Biochemical and Biophysical Research Communications* **376**, 723–727.
- Thaler JS, Fidantsef AL, Bostock RM.** 2002. Antagonism between jasmonate- and salicylate-mediated induced plant resistance: effects of concentration and timing of elicitation on defense-related proteins, herbivore, and pathogen performance in tomato. *Journal of Chemical Ecology* **28**, 1131–1159.
- Toome M, Randjävär P, Copolovici L, Niinemets Ü, Heinsoo K, Luik A, Noe SM.** 2010. Leaf rust induced volatile organic compounds signalling in willow during the infection. *Planta* **232**, 235–243.
- von Dahl CC, Hävecker M, Schlögl R, Baldwin IT.** 2006. Caterpillar-elicited methanol emission: a new signal in plant–herbivore interactions? *The Plant Journal* **46**, 948–960.
- War AR, Paulraj MG, Ahmad T, Buhroo AA, Hussain B, Ignacimuthu S, Sharma HC.** 2012. Mechanisms of plant defense against insect herbivores. *Plant Signaling and Behavior* **7**, 1306–1320.
- Wasternack C, Parthier B.** 2007. Jasmonate-signalled plant gene expression. *Trends in Plant Science* **2**, 302–307.
- Wasternack C, Song S.** 2017. Jasmonates: biosynthesis, metabolism, and signaling by proteins activating and repressing transcription. *Journal of Experimental Botany* **68**, 1303–1321.
- Wi SJ, Ji NR, Park KY.** 2012. Synergistic biosynthesis of biphasic ethylene and reactive oxygen species in response to hemibiotrophic *Phytophthora parasitica* in tobacco plants. *Plant Physiology* **159**, 251–265.
- Wildt J, Kobel K, Schuh-Thomas G, Heiden AC.** 2003. Emissions of oxygenated volatile organic compounds from plants. Part II: Emissions of saturated aldehydes. *Journal of Atmospheric Chemistry* **45**, 173–196.
- Yli-Pirilä P, Copolovici L, Kännaste A, et al.** 2016. Herbivory by an outbreaking moth increases emissions of biogenic volatiles and leads to enhanced secondary organic aerosol formation capacity. *Environmental Science and Technology* **50**, 11501–11510.
- Zas R, Moreira X, Sampedro L.** 2011. Tolerance and induced resistance in a native and an exotic pine species: relevant traits for invasion ecology. *Journal of Ecology* **99**, 1316–1326.
- Zhang L, Xing D.** 2008. Methyl jasmonate induces production of reactive oxygen species and alterations in mitochondrial dynamics that precede photosynthetic dysfunction and subsequent cell death. *Plant and Cell Physiology* **49**, 1092–1111.
- Zhang L, Zhang F, Melotto M, Yao J, He SY.** 2017. Jasmonate signaling and manipulation by pathogens and insects. *Journal of Experimental Botany* **68**, 1371–1385.
- Zhao KJ, Chye ML.** 1999. Methyl jasmonate induces expression of a novel *Brassica juncea* chitinase with two chitin-binding domains. *Plant Molecular Biology* **40**, 1009–1018.